Coalescing Cation Selectivity Approaches in Ionomers

Priyamvada Goyal, Ahmet Kusoglu*, and Adam Z. Weber*

***Corresponding Author: akusoglu@lbl.gov, azweber@lbl.gov**

Lawrence Berkeley National Laboratory, 1 Cyclotron Rd, Berkeley, CA 94720 USA

ABSTRACT: Inconsistent selectivity measures used in the literature to quantify an ionomer's preference for one ion over another make it challenging to compare uptake of different ions across studies. Preferential ion-partitioning, which leads to partially exchanged membranes, needs to be studied to gain a fundamental understanding of the nature of ion/membrane interactions as well as to begin to unravel how varying ion fractions, whether or not intentional, may affect the membrane's properties and thus durability and performance. In this focus review, we use Nafion as a prototypical example to explore partial exchange studies and codify the various literature experiments and theory into a comprehensive whole, enabling formation of ionomer databases. A few representative approaches to selectivity are dissected to identify the points of divergence between them as well as to re-examine the embedded assumptions therein. Lastly, modeling strategies for ion selectivity of the membrane are reviewed to arrive at and correlate fundamental ion properties to ionomer selectivity.

Partition coefficients, which quantify the distribution of a species across phases at equilibrium, can be employed to characterize ion-exchange processes in applications as diverse as membranes used to remove ionic impurities from water,[1–3] perovskites for photovoltaic cells that require defect passivation *via* cation substitution,[4,5] and ionomer separators in CO_2 electrolyzers and fuel cells.[6–8] The ion-exchange requirements of some applications further comprise various levels of distinctions between different ionic species: understanding selectivity of Na and K ionic channels to regulate propagation of nerve impulses in the brain;[9] measuring ionic activity of abundant ions such as Na, K, Ca, Mg in soil solutions and silica sols;[10,11] allowing charge-carrying protons across while blocking the redox vanadium cationic species through the separators of all-vanadium redox flow batteries.[12–14] Although partition coefficients are relevant in such applications, the ionic-species-discerning materials need a specialized coefficient to quantify their relative preference for different ions – referred to as a "selectivity coefficient" in this work.

Notwithstanding the differences in the choice of concentration measure used, it is widely understood that partition coefficients (or distribution coefficients) represent the ratio of species concentration in the two relevant phases.[15,16] However, interpretations of the selectivity-coefficient-like quantities do not cut across disciplines. Even though the lack of common language binding similar phenomenon in different fields is inconvenient, the more baffling issue is the vast inconsistency in selectivity coefficients reported for identical materials used in the same application across studies.[17–19] Selective ion uptake as well as ion transport are vital functions of ion-exchange polymers (ionomers) used as solid-polymer electrolytes in electrochemical applications.[20,21] This work focuses on reviewing and standardizing binary selectivity coefficients used to characterize cation-exchange ionomers (CEI) employed in energy-conversion devices.[22,23] The aim is to revisit the barebone framework on which the various selectivity coefficients hinge, while providing an explicit scheme to interconvert amongst them. The findings, methodologies, and approaches, although derived for a specific set of ionomers, remain applicable to all the above applications.

Electrochemical applications employ several classes of cation-exchange ionomers such as perfluorinated (Nafion, Flemion, Aquivion, 3M), non-fluorinated (PBI, SPEEK), or composite membranes, depending on the chemical, mechanical, and thermal needs of the systems.[24–26] Each class of ionomer can have further variations along the lines of chemistry (ion-exchange capacity, side-chain chemistry), pretreatment, thickness, and functional modifications in accordance with the purpose they serve in the device.[22,27] Insights into the fundamentals of cation-exchange thermodynamics and the standardization of its quantifying measures are universally applicable to all CEIs. Perfluorosulfonated acid (PFSA) membranes such as Nafion are one of the more commonly used CEIs, and the wealth of data on these materials and their ubiquity make them ideal for this review discussion. The polytetrafluoroethylene

backbone (hydrophobic) of Nafion has side chains that terminate in negatively charged sulfonic-acid moieties (hydrophilic). Hydration of ionic sites leads to phase-separated morphology in these membranes. Nafion performs the dual function of keeping the oxidizing and reducing electrode compartments separate while mostly only allowing current-carrying cations (counter-ions to the fixed anionic sites) to diffuse through. A proton's small size with high mobility and ability to form hydrogen bonds lend it the highest conductivity through the hydrophilic domain network of the ionomer. Lately, Nafion, in its thin-film form, has also been incorporated into the cathode catalyst layers of proton-exchange-membrane fuel cells and electrolyzers to facilitate enhanced proton conduction to reaction sites and thus mitigate the sluggishness of oxygen reduction reactions, thereby improving overall cell performance.[22,28,29]

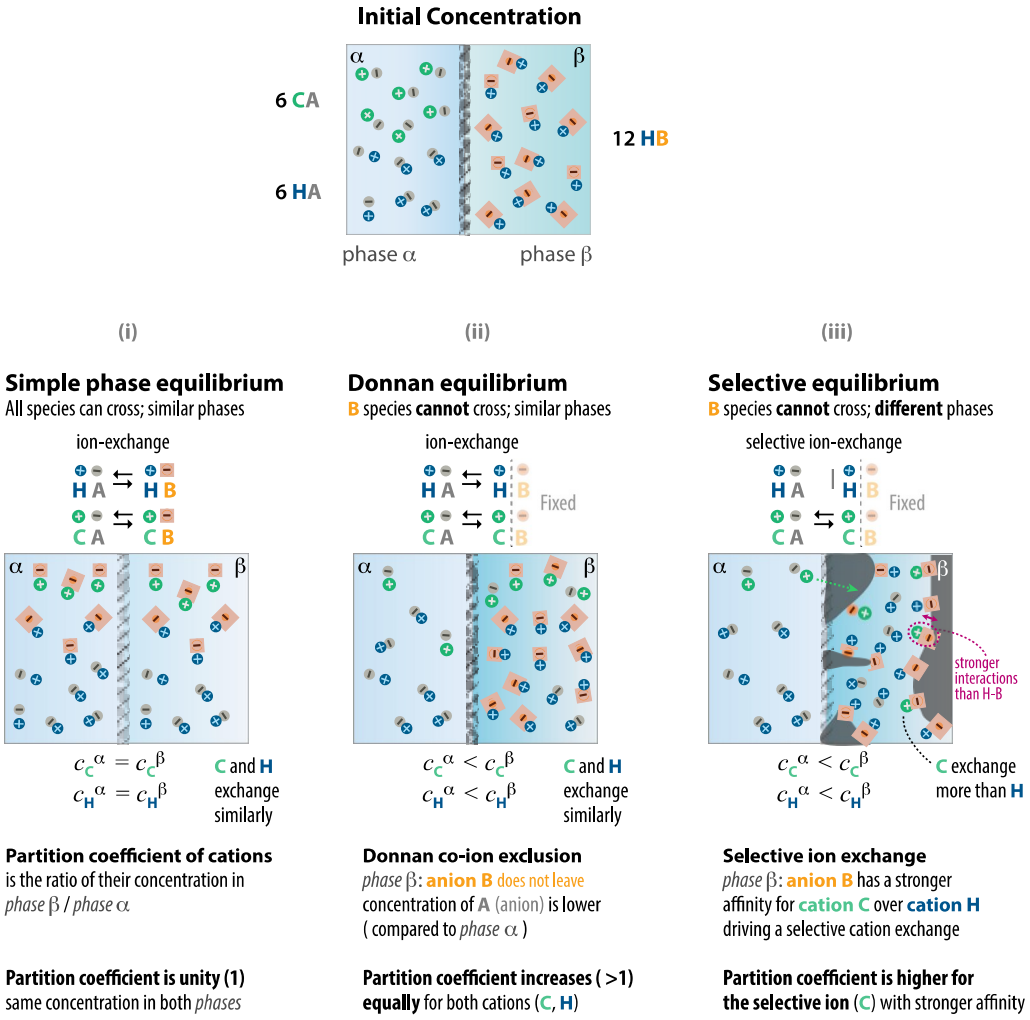

Figure 1. The schematic demonstrates the key differences between the various kinds of chemical equilibria that can exist between two phases (i) Simple phase equilibrium: leads to equal distribution of species across phases (ii) Ideal Donnan equilibrium: leads to partitioning of species across phases (iii) Nonideal Donnan or selective equilibrium: leads to preferential partitioning of one species over another across phases.

The interest in cation-exchange in Nafion has been renewed recently due to its selective transport functionality in redox flow batteries,[12,13,30] and the presence of cations other than protons, whether impurities or additives, in the fuel-cell environment.[31–33] One prominent example of the latter is the doping of Nafion and similar ionomer membranes for fuel cells with cerium.[34–37] Cerium ions prevent chemical degradation of PFSAs by scavenging free radicals that break down the backbone leading to fluoride emissions. Introduction of a multivalent ion like Ce, however, ends up displacing protons from the membrane to maintain bulk electroneutrality, thereby decreasing conductivity.[37] Unintentional cations such as Co, Pt, Fe can also enter the membrane-electrode-assembly through impure fuel streams, leaching from metallic cell components, or dissolution of catalyst metals and alloys.[22,32,38–40] Characterization of multi-ion uptake behavior in mixed-cation systems has been an underexplored dimension of ionomer research. While there are studies reporting sorption, transport, and mechanical characteristics of fully-exchanged (H, Na or other cation forms) PFSAs,[22,41–43] such investigations have not always been extended to partial

exchange of cations. The impact of contaminant and additive cations in ionomers on cell performance, however, requires analysis of partially exchanged PFSAs.[36]

Figure 1 lays out the fundamentals of partial cation-exchange from a ternary electrolyte, containing two cations, into another phase such as a membrane (note that although cations are emphasized here, the same cases and discussions are relevant for anion-exchange). All the ions are assumed to be fully dissociated for the purposes of this simple illustration. Based on the relative energetics of the two phases, equilibrium may lead to equal (case (i): simple equilibrium) or unequal distribution (case (ii): Donnan equilibrium [44] and case (iii): selective equilibrium) of species concentrations across the phases. In the unequal distribution cases, the concentrations of cations are different in the two phases, their ratio quantified as the *partition coefficient*. Often, one of the cations, possessing a higher partition coefficient, is preferentially partitioned into the membrane owing to its more favorable interactions with the membrane environment as in case 3; in other words, the membrane is found to be *selective* (relatively) towards one cation over the other. The few relevant partial-exchange studies of Nafion available in literature focus on the competitive uptake of protons with monovalent alkali metal ions from a ternary aqueous electrolyte.[45–47] Experimental data on transition metals and multivalent ions, in general, is relatively scarce, with some exceptions (See ref. 22 for a review of the topic).[17,19,39]

Apart from the shortage of experimental selectivity data for cations pertinent to fuel cells, a major challenge in understanding the cation selectivity behavior of ionomers emanates from the variety of approaches taken to quantify partition and selectivity. It is challenging to bring together the various experimental sources measuring partial-cation-exchange because they are neither consistent in how they quantify or even report selectivity. Various approaches taken to describe cation selectivity in ionomers include:

- qualitative assessment and comparison of ion partitioning data usually plotted as cation concentration in membrane *vs* cation concentration in the aqueous phase; Figure 2 is presented as a sample plot
- exchange fraction, *i.e.*, the ratio of the amount of a cation associated with the sulfonic acid sites to the maximum amount of the same cation in a fully-exchanged state (saturation fraction) in the membrane[37]
- binary selectivity coefficient, which can be expressed as a combination of the partition coefficients of two cations being compared[45,48]

Each approach presents its own issue with regard to consistency. Partitioning plots only provide qualitative comparison and may obscure the difference between simple and ideal Donnan equilibrium, depending on the composition measure used. For monovalent cations, exchange fractions also represent the fraction of the cations interacting with the polymer's fixed ionic groups. However, such representation fails for multivalent cations due to mismatch between the amount of mono- and multi-valent cations, as per electroneutrality. The variety of conventions used in defining binary selectivity coefficients makes the different reported values incompatible with each other. The effort to eliminate ambiguity in approaches to measure and quantify ion-exchange processes, although developed for a well-defined system of PFSA ionomers in fuel cells, would be beneficial to a wide variety of materials.

This standardization approach for selectivity measure quantification would foster more transparent communication between the theory, modeling, and experimental aspects of multi-ion partitioning. This paper aims to amalgamate the various theoretical approaches to quantify selectivity coefficients across literature so that the existing as well as new experimental data on Nafion cation selectivity can be processed together into one consistent database, paving the way to extend this methodology to other materials. Below, the theoretical inquiry reframes the thermodynamic origins of selectivity coefficients for the present context, facilitating systematic comparisons between the wide range of conventions used for selectivity coefficients, their relative merits, and the various assumptions that are usually hidden within them. Even though a detailed equilibrium model comprising key contributions to the ion-partitioning phenomenon, such as those developed by Bontha and Pintauro,[48] Crothers *et al,*[49] and Freeman *et al.,*[50] is the more quantitatively accurate way of evaluating a membrane's preference for a given ion from a multicomponent mixture, it is well worth developing a qualitative intuition about the likely relative sorption of one cation versus another. Therefore, correlations between cation fundamental properties and the selectivity coefficients measured for binary cation systems in Nafion are elucidated towards the end of this focus review.

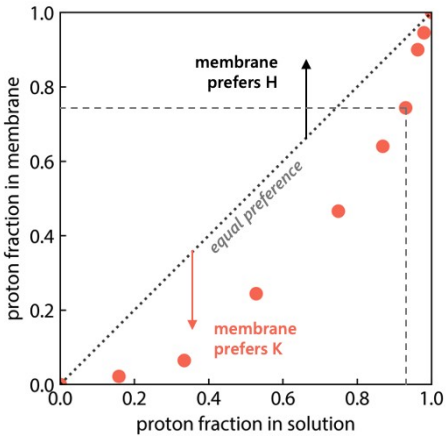

Figure 2. Typical partitioning plot with cation fraction uptake into the membrane plotted as a function of cation fraction in the external solution. The 45-degree line reflects a system with no preferential partitioning, depicting ideal Donnan equilibrium. Orange circles represent proton-potassium partitioning data into Nafion from an aqueous solution, taken from Okada and coworkers.[45] All the data points lie below the equal preference line denoting the preferential partitioning of potassium into Nafion over protons.

THERMODYNAMIC ORIGINS OF THE SELECTIVITY COEFFICIENT

Gibbs introduced the fundamental phase equilibrium laws in his seminal work "*On the Equilibrium of Heterogeneous Substances*" in 1876.[51] Since then, researchers in different fields have adapted his theory for their applications: Donnan applied the Gibbs' framework to understand biological membranes,[44] whereas Gaines and Thomas and others applied it towards describing ion-exchange phenomenon for clay minerals.[52–55] These works formed the foundational references for the theoretical treatment of ion-exchange physics in cation-exchange membranes in their respective fields. This section uses the same Gibbs' phase equilibrium framework.

Guggenheim defined the (electro)chemical potential of a species i, μ_i, as the change in Gibbs free energy, G, when a mole of charged species i is reversibly added to the system while keeping the amounts of other components as well as temperature, T, and pressure, p, constant,[56]

$$\mu_i = \left(\frac{\partial G}{\partial n_i}\right)_{T,p,n_{k\neq i}}. \quad (1)$$

For an uncharged species, this yields the chemical potential. The ion-exchange phenomenon between two phases, solution phase (s¿ and membrane phase (m), is governed by the thermodynamics of phase equilibrium ($dG=0$), expressed mathematically as,

$$\mu_i^s = \mu_i^m. \quad (2)$$

This condition is only applicable to a species i that is free to move between the two phases. Also, the conditions of thermal and mechanical equilibrium are implicit. Given that competitive partitioning of cations relative to protons into Nafion PFSA ionomers drives this work, the solution phase is assumed to be a ternary aqueous electrolyte containing two salts, one containing protons, H, and the other with a different cation, C, but both complexed with the same anion, A. This solution is in contact with the Nafion membrane embedded with bound anion sites, B, while species H, C, A, and water (0) are free to move across the phase boundary.

A mathematically convenient way to elucidate the characteristics of electrochemical potential is to express it in terms of species activity, a_i[57]

$$\mu_i = \mu_i^\theta + RT \ln a_i, \quad (3)$$

where R is the universal gas constant and μ_i^θ is the standard electrochemical potential of species i, which is a constant at a given temperature and pressure for any given phase. Although equation (3) is often applied to charged species, standard electrochemical potential for a single ion is not meaningful by itself. Furthermore, for a charged system, equation (1) hides the fact that changing the moles of only a charged species i (if that were practically possible) would alter the electrical state of the system.[58] The decomposition of electrochemical potential into its chemical and electrical contributions, however, is physically arbitrary.[59,60] This issue is circumvented here by adopting the Newman–Smyrl's

quasielectrostatic potential convention.[61] Protons are chosen to be the reference species and assumed to have ideal solution physics to define the potential Φ in each phase according to

$$\mu_H = RT \ln c_H + z_H F \Phi, \quad (4)$$

where F is Faraday's constant and c_i and z_i are the molar concentration and charge number (or valence) of species i, respectively. The condition of phase equilibrium can be applied to different species to yield information about the ion-exchange process. When applied to protons, $\mu_H^s = \mu_H^m$, it provides a way to calculate the potential difference between the two phases at equilibrium, $\left(\Phi^m - \Phi^s\right)$, commonly known as the Donnan potential,[44,59,62]

$$\Phi^m - \Phi^s = \frac{RT}{F z_H} \ln \frac{c_H^s}{c_H^m}. \quad (5)$$

The well-defined quasielectrostatic potential for the second cation, C, $\mu_C - \frac{z_C}{z_H}\mu_H$, can now be obtained by combining equation (3) applied to H and C,

$$\mu_C - \frac{z_C}{z_H}\mu_H = \left(\mu_C^\theta - \frac{z_C}{z_H}\mu_H^\theta\right) + RT\left(\ln a_C - \frac{z_C}{z_H}\ln a_H\right). \quad (6)$$

The condition of phase equilibrium for cation C is applied directly to the quasielectrostatic potential because it is a simple linear combination of potentials, μ_C and μ_H,

$$\mu_C^s - \frac{z_C}{z_H}\mu_H^s = \mu_C^m - \frac{z_C}{z_H}\mu_H^m. \quad (7)$$

Inserting equation (6) into equation (7) and rearranging to collect all the standard potentials on one side and all the activities on the other side yields,

$$K_{HC}^{eq} = \exp\left\{\frac{1}{RT}\left[\left(\mu_C^{\theta,m} - \mu_C^{\theta,s}\right) - \frac{z_C}{z_H}\left(\mu_H^{\theta,m} - \mu_H^{\theta,s}\right)\right]\right\} = \frac{a_C^s}{a_C^m}\left(\frac{a_H^m}{a_H^s}\right)^{\frac{z_C}{z_H}}. \quad (8)$$

The combination of activities on the right can be identified as the equilibrium constant, K_{HC}^{eq}, for an ion-exchange reaction of the form:

$$\frac{z_C}{z_H} H^s + C^m \rightleftharpoons \frac{z_C}{z_H} H^m + C^m. \quad (9)$$

The standard chemical potential is an arbitrary value facilitating the reporting of absolute values of chemical potential. Moreover, the standard electrochemical potential used for writing single-ion electrochemical potentials are impractical quantities because ions can only exist in solution unlike neutral compounds, solvents, etc. that can exist in pure states. This suggests that there may not be a reliable way to measure or estimate the equilibrium constant, K_{HC}^{eq}. The primary reference state (conditions at which the chemical potential reduces to the standard chemical potential) and the secondary reference state (conditions at which the species attains ideal behavior) are not independent of each other for solute species in electrolytic solutions. Newman and Balsara[59] resolve the above quandary by assuming the same secondary reference state for both the membrane and solution phase, which also ends up implying the same standard electrochemical potentials for species in both the phases. Under these constraints, K_{HC}^{eq} reduces to the value of 1, transforming equation (8) into

$$\frac{a_C^s}{a_C^m}\left(\frac{a_H^m}{a_H^s}\right)^{\frac{z_C}{z_H}} = 1 = \frac{c_C^s}{c_C^m}\left(\frac{c_H^m}{c_H^s}\right)^{\frac{z_C}{z_H}} \cdot \frac{\gamma_C^s}{\gamma_C^m}\left(\frac{\gamma_H^m}{\gamma_H^s}\right)^{\frac{z_C}{z_H}}. \quad (10)$$

The second equality in the relation above comes from recognizing that activity of a species contains more information than the concentration of the species, c_i. The effect of all the nonideal interactions of the species can be encapsulated in a quantity like the molar activity coefficient, γ_i. Thus, activity can be decomposed into

$$a_i = \gamma_i c_i . \quad (11)$$

Ideal solutions are defined by $a_i = c_i$ and $\gamma_i = 1$; positive deviations from ideality (unfavorable interactions that increase energy) yield $\gamma_i > 1$ and negative deviations (favorable interactions that decrease energy) yield $\gamma_i < 1$.

Equation (10) is the gateway to understanding membrane ion-selectivity although the aphysical nature (or unmeasurability) of single-ion activity coefficients dilutes its practical utility. It is possible to express equation (10) alternatively in terms of the measurable and meaningful quantities called "mean molar activity coefficients", γ_{ij},[59] defined for the neutral salt comprising oppositely charged species i and j,

$$\gamma_{ij}^{\nu_{ij}} = \gamma_i^{\nu_i} \gamma_j^{\nu_j} \vee (\gamma_{ij})^{\frac{1}{z_i}-\frac{1}{z_j}} = \gamma_i^{\frac{1}{z_i}} \gamma_j^{\frac{-1}{z_j}} . \quad (12)$$

where ν_i is the stoichiometric coefficient of ion i and $\nu_{ij} = \nu_i + \nu_j$. For the salt Na_2SO_4, $\nu_{Na^{+1}=2 \wedge z_{Na^{+1}}=1 ¿}$, $\nu_{SO_4^{2-1}=1 \wedge z_{SO_4^{2-1}}=-2 ¿}$ so that $\nu_{Na_2SO_4} = \nu_{Na^{+1}} + \nu_{SO_4^{2-1}=3 ¿}$. The Guggenheim relation for the formula unit for a salt $\sum_i z_i \nu_i = 0$ can be used to interconvert between ratios of stoichiometric coefficients and charge numbers.

With relation (12), equation (10) can be expressed in terms of the mean molar activity coefficients for neutral salts HA and CA, γ_{HA} and γ_{CA}, respectively in the solution phase and mean molar activity coefficients for the neutral cation combinations HB and CB formed with the membrane fixed anion species, B, γ_{HB} and γ_{CB}, instead of single-ion activity coefficients,

$$\frac{c_C^s}{c_C^m}\left(\frac{c_H^m}{c_H^s}\right)^{\frac{z_C}{z_H}} \cdot \frac{\left(\gamma_{CA}^s\right)^{1-\frac{z_C}{z_A}}}{\left(\gamma_{HA}^s\right)^{\frac{z_C}{z_H}-\frac{z_C}{z_A}}} \frac{\left(\gamma_{HB}^m\right)^{\frac{z_C}{z_H}-\frac{z_C}{z_B}}}{\left(\gamma_{CB}^m\right)^{1-\frac{z_C}{z_B}}} = 1 . \quad (13)$$

Based on molar concentration being the choice of composition made in equation (11), a molar binary selectivity coefficient, $S_H^{C,molar}$, can be defined by re-arranging equation (13) to

$$S_H^{C,molar} = \frac{c_C^s}{c_C^m}\left(\frac{c_H^m}{c_H^s}\right)^{\frac{z_C}{z_H}} = \frac{\left(\gamma_{HA}^s\right)^{\frac{z_C}{z_H}-\frac{z_C}{z_A}}}{\left(\gamma_{CA}^s\right)^{1-\frac{z_C}{z_A}}} \frac{\left(\gamma_{CB}^m\right)^{1-\frac{z_C}{z_B}}}{\left(\gamma_{HB}^m\right)^{\frac{z_C}{z_H}-\frac{z_C}{z_B}}} . \quad (14)$$

A different choice could have been made for defining activity in equation (11), such as $a_i = \Gamma_i m_i$, $a_i = \Gamma_i^y y_i$, or $a_i = \Gamma_i^x x_i$ where m_i, y_i, and x_i refer to molality, mole fraction, and cationic fraction of species i, respectively, whereas Γ_i, Γ_i^y, and Γ_i^x are the activity coefficients for the respective composition bases. The SI further elaborates on the relationship between different activity coefficients.

The use of the more popular bulk concentration measures, molarity and molality, in phase-separated materials such as Nafion to capture the physics of ion-exchange, which mostly occurs at the discrete charged sites, can be confusing. Detailed nanoscale models, typically implemented *via* molecular-dynamics simulations, that can resolve discrete charge sites are often only able to estimate probability distributions of cations across the pore, which are not true concentrations.[63,64] Characterizing ion-partitioning would require the actual cation concentration necessary to neutralize the total fixed-anion-site charge. The other strategy then is to use bulk concentrations but compute them locally to account for the expected gradient in cation concentration within the local hydrophilic domains, with concentration decreasing from the wall to the bulk of the domain. Thermodynamic models quantifying ion-exchange are given a continuum treatment; they tend to rely on average concentrations defined either on a superficial basis, *i.e.* on per unit volume or mass of membrane or on an interstitial basis, *i.e.* on per unit volume or mass of sorbed water in the membrane. Experimental methods to quantify ion exchange for a solid exchange membrane as well as the application of interest can also inform the concentration

measure used. In cases where exchanged cations from the membrane are leached into a solution to estimate their quantity, as is common, it is reasonable to interpret concentration as an average bulk quantity because the measurement itself does not have more nuanced information. The selectivity of the membrane can thus be interpreted as the difference in the total amount of the two absorbed cations without requiring knowledge of their distribution within the membrane. However, newer sophisticated techniques such as micro X-ray fluorescence and reflectivity allow for a more granular resolution of cation distribution where surface-site cation fractions are the more meaningful choice. Similarly, applications such as water purification that only care about the total amount of impurities removed from water by a membrane may continue relying on average concentration measures but they are not appropriate for applications where interfacial effects dominate such colloid science or thin-film ionomers in fuel cell catalyst layers. A summary of the different concentration measures used in cation partitioning literature is presented in Table 1 below.

Table 1. Concentration measures used in the context of ion partitioning into solid exchangers

Concentration measure	Definition	Material	References
Superficial molar concentration	moles/volume of wet exchange membrane	*Nafion*	40,48,65
Superficial molal concentration	moles/mass of dry exchange membrane	*Soils, Clays*	66,67
Interfacial molar concentration	moles/volume of hydrated domains in exchange membrane	*Nafion*	68,69
Cationic/Charge Fraction	amount of cation/amount of fixed anionic sites	*Nafion, Dowex, Clay, Glass*	10,11,45,46,70–73
Mole fraction	concentration of cation/total concentration of exchange phase	*Dowex, Sulphonic acid resins*	55,74

The fundamental physical interpretation of the selectivity coefficient would, however, remain largely unchanged with the choice of concentration measure used. The various composition variables and activity coefficients are laid out in a schematic in Figure 3 for ease of reference. Equation (14) is a key discussion of this review because it brings forth the theoretical basis of membrane selectivity—the fact that the two ions are partitioned into the membrane in a ratio different than they are present in the external solution.

There are two ways to evaluate the binary selectivity coefficient. The first approach is phenomenological and relies on the first equality relation in equation (14): measure the concentration of both cations in each phase at equilibrium to yield partition coefficients, $K_H = c_H^m / c_H^s$ and $K_C = c_C^m / c_C^s$. The absolute and relative magnitudes of these partition coefficients convey information regarding cation selectivity,

$$S_H^{C,\,molar} = \frac{K_H^{\frac{z_C}{z_H}}}{K_C}. \quad (15)$$

- $K_H^{z_C/z_H} = K_C$ implies that both the cations are partitioned equivalently into the membrane $\Rightarrow S_H^C = 1$
- $K_H^{z_C/z_H} > K_C \Rightarrow S_H^C > 1$, the membrane preferentially partitions protons H
- $K_H^{z_C/z_H} < K_C \Rightarrow S_H^C < 1$, the membrane preferentially partitions the second cation, C

The second approach examines the origin of selectivity and requires analysis of the second equality relation in equation (14) involving activity coefficients. It demonstrates that when the cations are dissimilar (in valence or other properties, $\gamma_H^{s/m} \neq \gamma_C^{s/m}$) as well as the phases are dissimilar (in their nonideal interactions leading to differing activity coefficients, $\gamma_{(H/C)}^{s} \neq \gamma_{(H/C)}^{m} \neq 1$), preferential partitioning of cations may occur across the phases. Note that this reasoning would hold even if the assumption of equilibrium constant, $K_{HC}^{eq} = 1$ was relaxed.

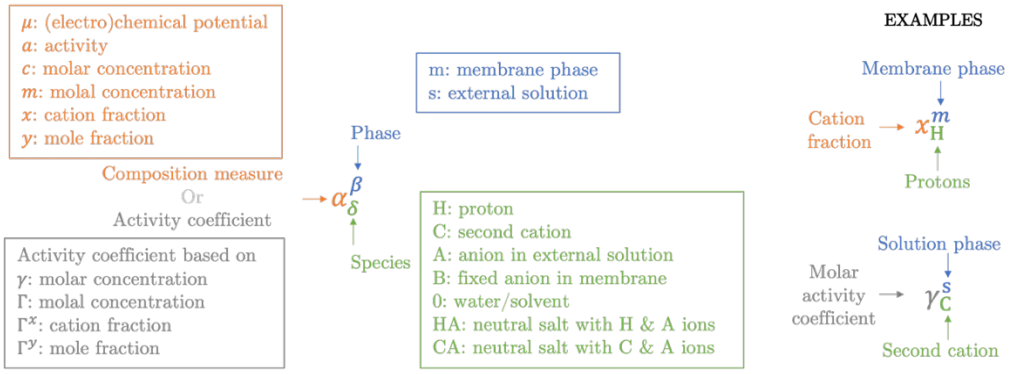

Figure 3. Pictorial dictionary to understand the variables nomenclature employed in the paper

RECONCILING SELECTIVITY COEFFICIENT MEASURES FROM LITERATURE

One of the peculiarities in reporting a selectivity coefficient in general is that, unlike an equilibrium constant, which is a fixed value at a given temperature, the selectivity coefficient often tends to vary with species composition. However, more often than not, a single selectivity value is reported in the Nafion literature. Although some groups are forthcoming about their convention for choosing a value, such as reporting the selectivity coefficient when half of the membrane sites are associated with protons [*Steck & Yeager*][19,46] or reporting the average value over the composition range [*Hongsirikarn et al.*][17], it is not always the case. Okada and coworkers[18,39,45] report a single value (with an error range) but do not explicitly state the convention. Pintauro et al.[48,68] and Crothers et al.[49] refrained from reporting a single value altogether, focusing instead on the composition dependence of the coefficient itself; a similar trend of reporting selectivity as a function of composition was seen in other fields as well.[67,75] Details of and comparisons among different conventions used for Nafion are included in the SI. A single-valued selectivity coefficient, which may be a pragmatic tool for facile comparison of different systems, can also be obtained by performing a nonlinear fit of experimental partitioning data for various cations based on a selectivity measure. In Figure 4, we fit (solid lines) the experimental cation partitioning data (markers) for Nafion [13,18,39,45,76,77] using Okada and coworkers' nonlinear selectivity coefficient expression,[45]

$$S_H^{C,Ok} = \left(\frac{x_H^m}{x_H^s}\right)^{\frac{z_C}{z_H}} \frac{x_C^s}{x_C^m}. \quad (16)$$

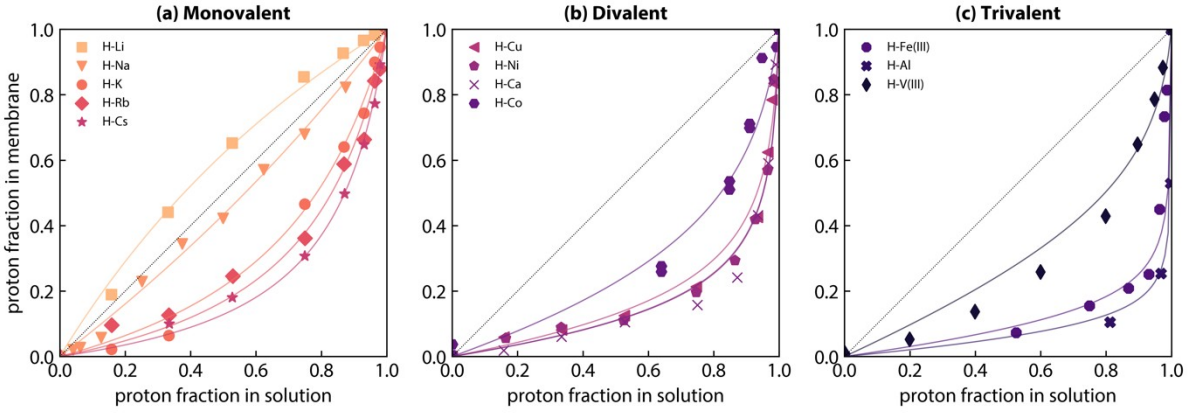

Figure 4. Nonlinear curve fits for selectivity coefficient grouped by valence (a) H/C^{+}, (b) H/C^{2+}, and (c) H/C^{3+}. The markers show experimental data [Li,Na,K,Rb,Cs: ref [45]; Cu,Ni,Fe: ref [39]; Ca: ref [18]; Co: ref [76]; Al: ref [77]] while the solid lines denote the nonlinear fits based on the Okada measure, equation (16). The grey 45-degree lines in all the plots denote the no preferential partitioning condition.

Table 2 lists the comparison of selectivity coefficients obtained from Okada and coworkers' selectivity data by applying the various conventions for a few representative cations. Although the different conventions produce comparable selectivity values for the monovalent ion (variation up to 13.5%), the disparity between conventions becomes starker as the cation valence increases (variation in divalent and trivalent ion up to 79.3% and

333.3%, respectively). Selectivity obtained from nonlinear data fitting consistently matches the order of magnitude of reported values in Okada papers across all valences.

Table 2. Comparison of selectivity coefficient reporting conventions using data from Okada and coworkers[39,45]

Ion/Ion Pair	Second cation valence	Reported (Okada)	Average (Hongsirikarn convention[17])	At $x_H^m = 0.5$ (Steck convention[19])	Non-linear Fit (This work)
H^+/Li^+	1	1.85 ± 0.16	1.82	1.62	1.63
H^+/Cu^{2+}	2	0.029 ± 0.010	0.052	0.029	0.039
H^+/Fe^{3+}	3	0.003 ± 0.002	0.012	0.013	0.003

As can be seen from the plots in Figure 4, Li is the only cation that is less preferentially partitioned into Nafion, as compared to protons. Comparison of Figures 4a, 4b, and 4c show that as the valence of second cation increases, it becomes progressively more strongly partitioned into the membrane, as evidenced from the increasing deviation from the equal partitioning 45-degree grey line on the plots. The nonlinear fits (solid lines) fit the experimental data (filled markers) well for cations of all valences.

A major challenge in reviewing ion-partitioning literature lies in reconciling the various measures used to quantify it, with the similarities in approaches further obscured by incompatible and inconsistent terminology. Selectivity coefficients can turn out to be quite distinct based on a few choices, namely: the composition measures used, whether nonideal interactions in the phases are included in the expressions, and the direction and stoichiometry of the ion-exchange reaction. These choices often relate to how the experiments were conducted without consideration of the underlying theoretical considerations discussed above. Thus, comprehending and comparing selectivity data across literature is cumbersome.

Table 3 lists selectivity coefficients reported for a variety of proton/cation combinations by Okada and coworkers,[18,39,45] Steck and Yeager,[19,46] and Hongsirikarn et al.[17] for Nafion of nominally similar ion-exchange capacities. The divergence in the quantitative coefficients, especially for multivalent cations, reflects the massive differences in processing and reporting of experimental data. Values reported for proton combinations with monovalent ions fall in the same order of magnitude. However, for the divalent cation Ca^{2+}, values differ by several orders of magnitude in the three sources consulted, $O(10^0)$ [Steck][19,46] vs $O(10^{-2})$ [Okada][18,39,45] vs $O(10)$ [Hongsirikarn];[17] a similarly drastic difference is seen for the H^+/Fe^{3+} combination as well. The remaining part of the section lays out the underlying dissimilarities in the various coefficients and then works on resolving them.

Table 3. Comparison of binary selectivity coefficient values for proton/cation combinations reported by multiple sources. Note that Nafion membrane-type differed across studies.

Ion/Ion Pair	Second cation valence	Steck[19,46]	Okada[18,39,45]	Hongsirikarn[17]
		Nafion 120	*Nafion 117*	*Nafion 211*
H^+/Li^+	1	0.586	1.85 ± 0.16	--
H^+/Na^+	1	1.18	0.73 ± 0.17	0.84 ± 0.08
H^+/K^+	1	3.48	0.25 ± 0.06	--
H^+/Rb^+	1	4.71	0.20 ± 0.07	--
H^+/Cs^+	1	7.06	0.14 ± 0.07	--
H^+/Ca^{2+}	2	2.87	0.021 ± 0.007	90.6 ± 38.6
H^+/Fe^{3+}	3	--	0.003 ± 0.002	4848 ± 1190

Table 4 collates the treatments for binary selectivity coefficients from five distinct sources in the literature. The divergence begins at the terminology employed to quantify the membrane's tendency of preferential cation partitioning. The selectivity measure expressions listed next make apparent the underlying reasons for differences in the numerical values of selectivity coefficients in Table 3. Apart from the difference stemming from reporting convention choice, the divergence among coefficients can be rationalized along the following dimensions:

- ***Direction of the ion-exchange reaction***: Okada's and Crothers' choices frame the second cation, C, in the membrane getting replaced with protons as the desired exchange, whereas the other three choose the opposite.
- ***Stoichiometry***: Okada and Hongsirikarn report selectivity per unit of the second cation exchanged (z_C/z_H exponent), whereas Steck and Crothers base it on per unit of proton exchanged (z_H/z_C exponent). Pintauro's expression is a direct ratio of the two cations' partition coefficients (no exponent).
- ***Composition variable used in each phase***: Okada and Hongsirikarn use cation fractions ($x_i^{m/s}$), Pintauro uses molar concentrations ($c_i^{m/s}$), and Crothers uses mole fractions ($y_i^{m/s}$) in both phases. Steck chooses mixed compositions—cation fractions in the membrane phase (x_i^m) but molar concentrations in the solution phase (c_i^s). All selectivity coefficients are dimensionless, however.
- ***Phase nonideality***: Steck's and Hongsirikarn's selectivity coefficients include solution-phase nonideality through molar (γ_i^s) and cationic fraction (Γ^{xs}_i) activity coefficients respectively. Based on equation (14), these selectivity coefficients end up measuring the relative nonideality of the two cations only in the membrane phase. The other selectivity coefficients (Okada, Pintauro, and Crothers) quantify the relative nonideality of the species in both the phases.

Identifying the various ways in which the measures differ allows for systematic interconversion among them, as elucidated in the last column of Table 4. Okada and coworkers have the most extensive data sets for binary ion partitioning (relative to protons) into Nafion membranes; therefore, their measure was chosen as the baseline. Although information in Table 4 is sufficient to allow conversions between any of the included measures, a more comprehensive version (Table S1) explicitly stating all the conversions is included in the SI. The nomenclature schematic in Figure 3 can be used as a reference to understand the various terms used in Table 4. Examination of the entries demonstrates the role of valence: all the conversions [equations (22)–(25)] simplify considerably if the valence of the two cations is the same, *i.e.*, $z_H = z_C$. For this case, Okada and Crothers measures become equivalent $S_H^{C,Cr} = S_H^{C,Ok}$, Pintauro measure is simply the reciprocal of Okada $S_H^{C,Cr} = 1/S_C^{H,Pin}$, whereas Steck and Hongsirikarn measures differ from the reciprocal of the Okada measure by ratio of the activity coefficients of the two cation, $S_C^{H,St} S_H^{C,Ok} = \gamma_H^s/\gamma_C^s$ and $S_C^{H,Hon} S_H^{C,Ok} = \Gamma^{xs}{}_H/\Gamma^{xs}{}_C$ respectively. This is the reason selectivity values for monovalent cations in Table 2 look comparable, but they diverge as the difference in valence of the two cations increases.

Table 4. Summary of terminology and different selectivity measures used across literature. For each source, the specific form of the ion-exchange reaction which forms the basis of that measure is also included. The last column of the table lists conversion from the Okada measure to all the other measures. Figure 3 describes the symbols used in this table.

	Ion-exchange Reaction / Selectivity Measure		Conversions from Okada, $S_H^{C,Ok}$	
Okada[18,39,45] *Equilibrium constant for the exchange reaction*	$\frac{z_C}{z_H}H^s + C^m \rightleftharpoons \frac{z_C}{z_H}H^m + C^s$ $S_H^{C,Ok} = \left(\frac{x_H^m}{x_H^s}\right)^{\frac{z_C}{z_H}} \frac{x_C^s}{x_C^m}$	(17)	$S_H^{C,Ok} = S_H^{C,Ok}$	
Steck[19,46] *Selectivity coefficient*	$H^m + \frac{z_H}{z_C}C^s \rightleftharpoons H^s + \frac{z_H}{z_C}C^m$ $S_C^{H,St} = \frac{c_H^s \gamma_H^s}{x_H^m}\left(\frac{x_C^m}{c_C^s \gamma_C^s}\right)^{\frac{z_H}{z_C}}$	(18)	$S_C^{H,St} = \frac{1}{\left(S_H^{C,Ok}\right)^{\frac{z_H}{z_C}}} \frac{\frac{\gamma_H^s}{z_H}}{\left(\frac{\gamma_C^s}{z_C}\right)^{\frac{z_H}{z_C}}} \left(-z_A c_A^s\right)^{1-\frac{z_H}{z_C}}$	(22)
Pintauro[47,48,68] *Selectivity*	$H^m + C^s \rightleftharpoons H^s + C^m$ $S_C^{H,Pin} = \frac{c_H^s}{c_H^m}\frac{c_C^m}{c_C^s}$	(19)	$S_C^{H,Pin} = \frac{1}{S_H^{C,Ok}}\left(\frac{x_H^m}{x_H^s}\right)^{\frac{z_C}{z_H}-1}$	(23)
Hongsirikarn[17] *Equilibrium exchange constant*	$\frac{z_C}{z_H}H^m + C^s \rightleftharpoons \frac{z_C}{z_H}H^s + C^m$ $S_C^{H,Hon} = \left(\frac{x_H^s \Gamma_H^{xs}}{x_H^m}\right)^{\frac{z_C}{z_H}} \frac{x_C^m}{x_C^s \Gamma_C^{xs}}$	(20)	$S_C^{H,Hon} = \frac{1}{S_H^{C,Ok}}\frac{\left(\Gamma_H^{xs}\right)^{\frac{z_C}{z_H}}}{\Gamma_C^{xs}}$	(24)
Crothers[49] *Absorption nonideality parameter*	$H^s + \frac{z_H}{z_C}C^m \rightleftharpoons H^m + \frac{z_H}{z_C}C^s$ $S_H^{C,Cr} = \frac{y_H^m}{y_H^s}\left(\frac{y_C^s}{y_C^m}\right)^{\frac{z_H}{z_C}}$	(21)	$S_H^{C,Cr} = \left(S_H^{C,Ok}\right)^{\frac{z_H}{z_C}}\left(\frac{z_A y_A^s}{z_B y_B^m}\right)^{\frac{z_H}{z_C}-1}$	(25)

Table 5. Thermodynamic relationships characterizing the membrane phase; superficial molar concentrations are used.

KNOWN

Measured quantities

Membrane water content

$$\lambda = \frac{c_0^m}{c_B^m} \quad (26)$$

Cation fraction

$$x_H^m = \frac{z_H c_H^m}{z_H c_H^m + z_C c_C^m} \quad (27)$$

Thermodynamic relations

Equation of state

$$V_0 c_0^m + V_B c_B^m = 1 \quad (28)$$

(ignore ionic volumes)

Additional constraints

Cation-fraction sum

$$x_H^m + x_C^m = 1 \quad (29)$$

Bulk electroneutrality

$$z_H c_H^m + z_C c_C^m + z_B c_B^m = 0 \quad (30)$$

(ignore co-ion uptake)

Definitions

Mole fraction

$$y_i^m = c_i^m / c_T^m \quad (31)$$

Total concentration

$$c_T^m = c_0^m + c_H^m + c_C^m + c_B^m \quad (32)$$

DERIVED

Molar concentrations

$$c_B^m = \frac{1}{V_0\lambda + V_B} \quad (33)$$

[combining 28 and 30]

$$c_0^m = \frac{\lambda}{V_0\lambda + V_B} \quad (34)$$

[combining 28 and 35]

$$c_H^m = -\frac{z_B}{z_H}\frac{x_H^m}{V_0\lambda + V_B} \quad (35)$$

[combining 29, 31, and 34]

$$c_C^m = -\frac{z_B}{z_C}\frac{x_C^m}{V_0\lambda + V_B} \quad (36)$$

[combining 30, 31 and 34]

$$c_T^m = \frac{1 + \lambda - z_B\left(\frac{1-x_H^m}{z_C} + \frac{x_H^m}{z_H}\right)}{V_0\lambda + V_B} \quad (37)$$

[combining 31, (33)–(36)]

The interconversions, as noted in equations (22) through (25), involve several quantities. Some of them may be directly available from partitioning experiments themselves (cation fractions of protons, $x_H^{s/m}$ and external anion concentration c_A^s, y_A^s), some others can be estimated from theory even though they are not physically accessible quantities (single-ion activity coefficients, γ_i^s, $\Gamma^{xs}{}_i$), and the remaining can be calculated from thermodynamic and electrochemical relations governing system behavior (mole fractions of bound sites in the membrane, y_B^m). In addition to defining several composition measures, Table 5 summarizes the thermodynamic equations of states, bulk electroneutrality constraints, and some equilibrium properties of the phases that constitute the mathematical framework necessary to arrive at and numerically implement the interconversions among the various partitioning quantifiers listed in Table 4. The calculations in Table 5 assume that even though co-ions, which are anions A in this system, can get partitioned into the membrane, experiments show their uptake to be quite small in comparison to the cation and water uptake (due to Donnan exclusion) under these lower concentration conditions (*i.e.*, low ionic strength).[17,45] Hence, co-ion charge density and concentration are ignored in the bulk electroneutrality (equation (30)) and total concentration (equation (32)) for the membrane phase, respectively.

Although Table 5 does not explicitly show mole fractions, we can easily derive these from molar concentration equations (33)–(37). For instance, applying equation (31) to the bound species B in the membrane along with equations (33) and (37) yields the mole fraction of B,

$$y_B^m = \frac{1}{1+\lambda - z_B\left(\frac{1-x_H^m}{z_C}+\frac{x_H^m}{z_H}\right)}, \quad (38)$$

which can then be used in equation (25) to convert the Okada's selectivity measure to Crothers'.

Tables 4 and 5 interpret bulk concentrations and therefore selectivities to be superficial (i.e. on a wet membrane volume basis) but superficial selectivities can be converted to the interstitial basis by accounting for the water phase volume fraction in the membrane,

$$S_i^{j,\text{¿}} = S_i^{j,\int \text{¿}\phi_0^{\frac{z_j}{z_i}-1}\,\text{¿}} \quad (39)$$

The conversion from interstitial to superficial selectivity exhibits the role of membrane swelling in selectivity calculations. Some other measures, such as cation fractions, seem independent of membrane water uptake but other measures such as molarity or mole fractions explicitly depend on it. Water uptake should be solved simultaneously with ion uptake through phase equilibrium calculations since they are coupled variables; water uptake of Nafion is a function of counter-ion type. For instance, Nafion swells much less in Cs^+ form than in Na^+ form.[41]

Converting from Okada to Steck measure: an example

The interconversion expressions from Table 4 along with the knowledge of reporting conventions used by different sources make it possible to meaningfully carry out the conversion from one selectivity measure to another. The schematic in Figure 5 illustrates the process for the particular case of converting from Okada to Steck measure in detail, generally as well as for the specific case of the membrane exposed to a solution of HCl and LiCl. First, based on partitioning data from Okada,[45] selectivity coefficients, calculated using equation (16), are calculated for each combination of solution-membrane proton fraction. Single-ion activity coefficients for the cations are obtained from Kielland [79] at the ionic strengths used by Steck.[19,46] The anion concentration in the solution phase is computed based on the same ionic strength information coupled with the bulk electroneutrality condition and cationic fraction definitions. Finally, a single value for Steck selectivity coefficient is reported for $x_{HM} = 0.5$, following Steck convention.

Steck selectivity coefficient values for alkali metal and Ca^{2+} cations as reported by Steck and those converted from Okada to Steck, following Figure 5, are included in Table 6. Even though the membrane types (Nafion 117 for Okada and Nafion 120 for Steck) and pretreatment conditions vary between the two studies, good agreement is obtained between the selectivity coefficient values. The correct orders of magnitude of the converted values reflect the usefulness of the approach. Note that it is important to use the solution strengths (to obtain external anion concentration and activity coefficients) and reporting conventions of the target measure (Steck in this case) to achieve a close match. Although Nafion 120 (250 micrometers) is thicker than Nafion 117 (178 micrometers), this difference is unlikely to affect an equilibrium measurement such as ion sorption. Further, the small difference of 100 g/eq in equivalent weights of the two membranes, ~1200 g/eq for Nafion 120 vs ~1100 g/eq for Nafion 117, should not be sufficient to cause a significantly different local environment for cations interacting with the membrane phase. Therefore, it is reasonable to compare the selectivity values of the two different membranes.

Table 6. Steck selectivity coefficient values for different ion combinations as reported by Steck[19] for expanded form Nafion 120 compared to the values obtained from converting the Okada[18,45] data for Nafion 117.

Ion/Ion Pair	Second cation valence	Reported (By Steck)	Converted (From Okada)
H^+/Li^+	1	0.586	0.623
H^+/Na^+	1	1.18	1.32
H^+/K^+	1	3.48	3.54
H^+/Rb^+	1	4.71	4.99
H^+/Cs^+	1	7.06	6.95
H^+/Ca^{2+}	2	2.87	3.53

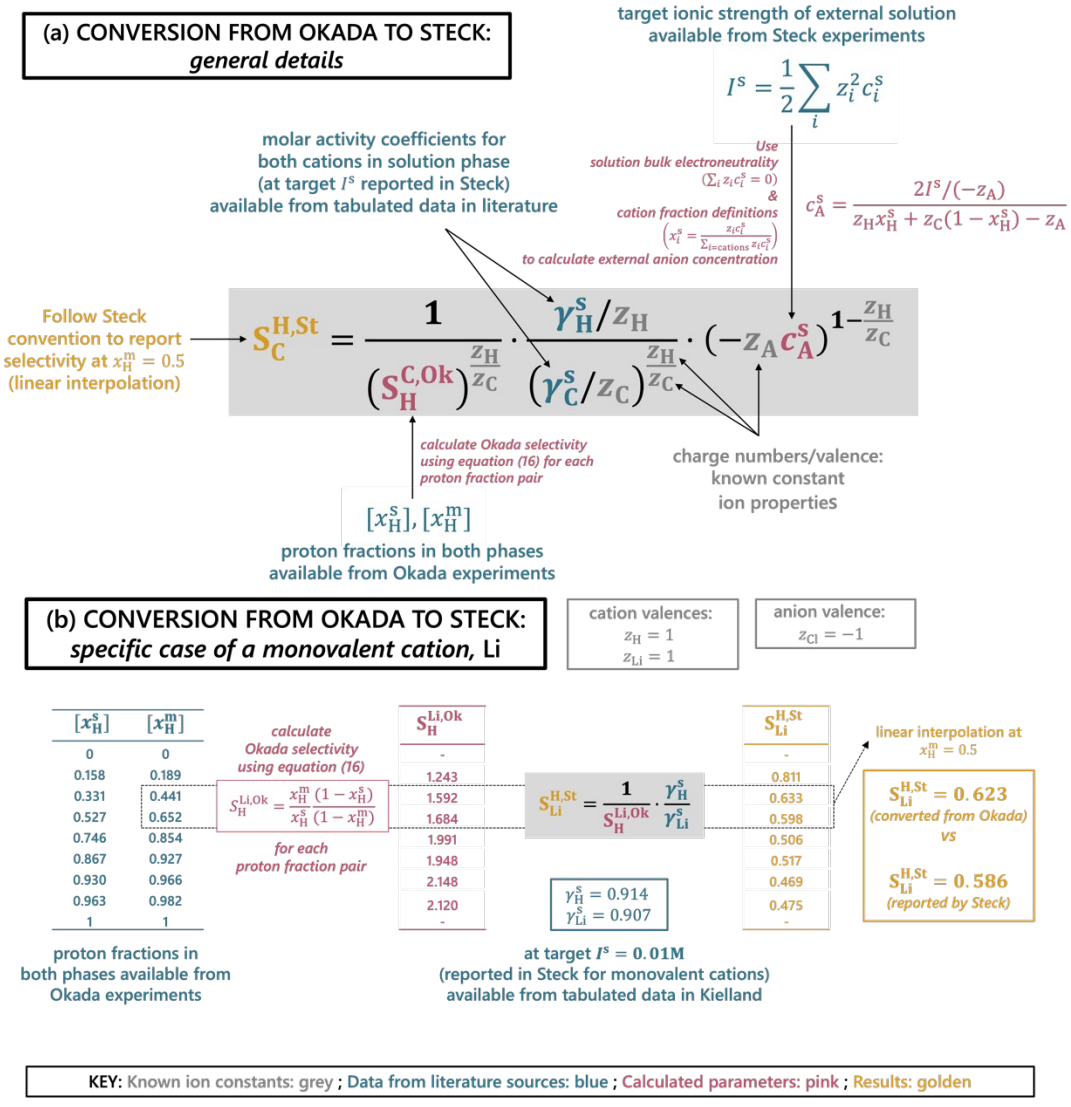

Figure 5. (a) Schematic detailing how to obtain the various quantities involved in equation (22) to convert from Okada to Steck selectivity measure. Quantities directly reported in literature are shown in blue emanating from different sources: Okada, Steck, Kielland.[19,45,79] Calculated quantities (and the related math) are shown in a shade of pink. The final quantity, Steck selectivity coefficient, is shown in golden. The known constants are shown in dark grey. (b) Specific example for the conversion of selectivity value for H/Li is included to further clarify the process. The molar activity coefficients for protons and lithium are obtained from the tabulated data in Kielland.[79]

EXPLORING CORRELATIONS BETWEEN SELECTIVITY AND CATION PROPERTIES

The thermodynamic equilibrium analysis above traced the origins of binary cation selectivity behavior to different interactions of the two cation species in the phases concerned. Experimental data, discussed thereafter, provides a way to estimate directly the consequence of said interactions, typically nonideal, by measuring concentrations of different species in the phases. However, concentration data does not directly shed any light on the specific nature of the nonideal interactions or the fundamental physics that engenders them. Ideal Donnan theory,[44] ubiquitously used to describe ion-partitioning into membranes, is unable to capture selective ion-partitioning behavior of membranes on its own. Theoretical models for the activity coefficients (measures of deviation from ideality) of salt species in the two phases are necessary to fill this gap. Many well-established models exist to quantify the nonideal interactions in electrolyte solutions[56,80] but models for activity coefficients in the membrane phase are comparatively rare. One approach is to base the hydrophilic region physics in the membrane on electrolyte solutions with some modifications unique to the membrane phase, such as accounting for ion-pairing between fixed-charge-sites on the membrane and the absorbed counter ions[48] or adding a swelling pressure contribution.[49] Another approach is more polymer-physics centric where Flory–Huggins–Rehner theories[62,81] and Manning's counter-ion condensation theory [50,62,82] are used to model complex interactions in the ionomer (See review [83] for an overview of the various modelling approaches to ion sorption in membranes). These models produce reasonable matches with experimental data, albeit under limited conditions. For instance, some of these models are yet to expand to multicomponent solutions,[84] while some include parameters that are not straightforward to measure independently.[36,43] This negatively affects the predictive capability of the models and perhaps even sound physical interpretability of the model parameters. It is, therefore, worthwhile to explore correlations between a phase's cation selectivity and some fundamental phase or cation properties that are likely to control its interactions with the surrounding environment, as a complementary qualitative measure to the quantitative models.

The theoretical models are leveraged to glean cation properties that might be relevant to phase nonideality. Given that Coulomb's law (force between two charges $\propto z_i z_j / r_{ij}^2$) forms the basis of an ion's electrostatic interaction with its surroundings (*via* Debye–Hückel theory)[59], cation valence (z_C ¿ and its unsolvated ionic radius (r_C ¿[85,86] emerge as non-controversial fundamental properties of interest. Properties that may inform a cation's interactions with water may include hydrated radius, r_C^{hyd} [86] and hydration enthalpy, ΔH_C^{hyd}. [87] Similarly, short-range specific ion/ion effects can be imagined to be associated with a cation's Lewis acid strength (LAS_C) [88,89] and electronegativity (χ_C). [90,91] Ionomer mechanical properties such as bulk modulus ($E_{mem,C}^{dry}$) and morphological properties such as domain spacing (d_C), which contribute to swelling and steric effects respectively, may also be affected by cation-type[41] but are not included in the current study due to insufficient experimental data for membranes in different cation-forms.

The SI systematically studies correlations among cation fundamental properties to avoid running into the issue of multicollinearity – high degree of correlation among independent properties that results in untrustworthy correlations between dependent and independent variables. Strong correlations were observed between hydration-related properties ($r_C^{hyd} \wedge \Delta H_C^{hyd}$) and combination of cation valence and radius that can be interpreted as charge density-like variables ($z_C / r_C \wedge z_C^2 / r_C$, respectively). The correlation between hydration enthalpy and charge density follows from an effective-medium theory approach where energy released from the interaction between a cation (point-charge) and a solvent (continuum electrostatic field) is expressed by combining the differential form of Gauss's law (electric flux density originates from the volume charge density at any point in space) with Coulomb's law. Although correlations for electronegativity (χ_C) and Lewis acid strength (LAS_C) with the charge-density-like variables were not as firmly based in theory, they were still too strong to be overlooked. Therefore, unsolvated ionic radius r_C, and charge density z_C^2 / r_C, are the only independent variables considered for this study.

Figure 6 shows correlations between binary selectivity coefficients of protons relative to a second cation and the selected fundamental properties of that cation: if selectivity >1, Nafion is more likely to uptake proton instead of the second cation. Further, for example $S_H^{Rb} > S_H^{Cs}$ implies that Nafion is more selective towards Cs over Rb. The selectivity coefficient values are based on Okada's measure since their orders of magnitude clearly follow cation valence, as can be seen from the banded nature of the selectivity values on the log scale. Although Okada and co-

workers reported selectivity for many ions across valences, as reported in Table 1, meaningful correlation analysis required more data points. Partitioning data for other cations are reported in a few sources in the literature: monovalent: Ag, Tl; divalent: Mg, Sr, Ba, Co, Zn from Steck[19] and trivalent: Al from Prakash[77] and V(III) from Zawodzinski.[14] The interconversion methodology described in the previous section was put to use to convert all selectivity coefficients to the Okada measure. Steck directly reported selectivity coefficients without the partitioning data, therefore it is difficult to apply any other reporting convention to their coefficients. Therefore, for the sake of consistency, Steck convention of reporting selectivity at $x_{HM}=0.5$ was adopted for all the ions. This exercise helped start building a cation selectivity database for Nafion, as shown in Table 7.

The top row of plots in Figure 6 (a–c) does not group cations according to any classification whereas the bottom row (d–f) groups them according to their valence. The top and bottom plots for the two independent variables, r_C and z_C^2/r_C, tell very different stories, demonstrating the notorious Simpson's paradox. Simpson's paradox, *i.e.* change in correlation with grouping of data, can be explained by way of an example: plot 6b shows a moderately strong negative correlation between selectivity and z_C^2/r_C that can lead to the conclusion that membrane selectivity towards protons decreases as the charge density of the second cation increases. However, upon grouping by valence, Figure 6e shows that for a given valence, the selectivity for protons increases as charge density increases; the second correlation implies that protons should be more favored over the high-charge-dense K than the low-charge-dense Cs, which we know to be true from experiments. Therefore, grouping data according to valence yields more accurate correlations. No trends were obtained for trivalent ions on their own because of insufficient data.

The grouping according to cation valence is uncontentious for ionic radius. However, given that charge-density z_C^2/r_C already contains a valence dependence within its definition, an additional valence-dependent feature complicates its analysis. Furthermore, the charge-density correlation does not offer any new information beyond what is contained in the ionic radius plot. For a given valence, selectivity becomes a function of ion size: Nafion is more selective towards larger cations. For a given ionic radius, selectivity becomes a function of ion valence: Nafion is biased towards multivalent cations. These observations led to the semi-empirical functional form involving r_C and z_C explored in plots 6(c) and 6(f):

$$S_H^C \propto \exp(a r_C)\exp(b z_C). \quad (40)$$

This form collapses the plots for different cation valence shown in plots 6(a) and 6(d) onto one single correlation, a feature that makes it significantly more useful. Note that this form does away with Simpson's paradox, allowing for a more straightforward analysis. Additionally, equation (40) reiterates that size and charge effects are decoupled. Plot 6(c) makes a statement of great utility: knowledge of the second cation's valence and ionic radius should be sufficient to deduce its approximate binary selectivity coefficient with respect to protons. This hypothesis can be tested over time as partitioning data for new cations is acquired.

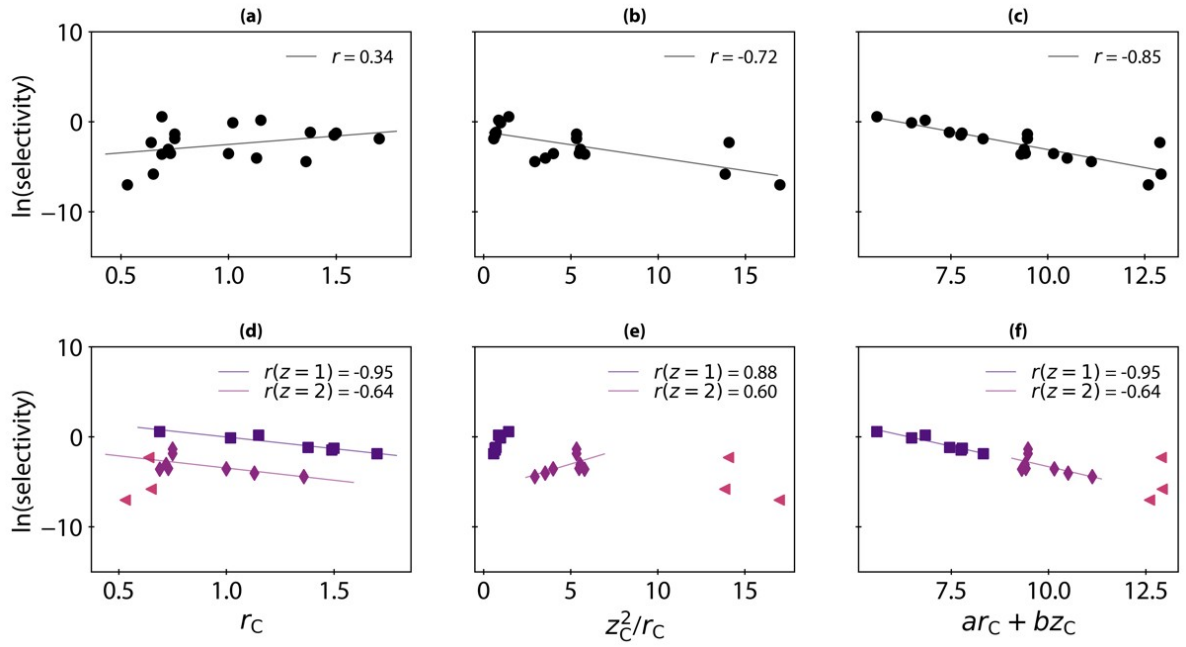

Figure 6. Correlation plots for cation fundamental properties with proton-cation selectivity coefficients. Selectivity coefficients follow Okada measure [ref. equation (16)] and Steck reporting convention [ref. Table 1]. Subplots (a)–(c) plot selectivity values of Nafion membrane for protons relative to other cations [circles (●)] as a function of cation radius, r_C charge density, z_C^2/r_C and a combination of the two, $a\,r_C + b\,z_C$, respectively. Subplots (d)–(f) plot the same data as (a)–(c) while differentiating between cation valence to explore trends in selectivity behavior; monovalent cations: square (■), bivalent cations: diamond (♦), trivalent cations: triangles (◂). The solid lines in all the plots are linear fits of the corresponding colored marker data, with correlation coefficient, r, noted for each fit. Subplots (c) and (f) show an empirical universal relation between ln(selectivity), cation radius r_C and cation charge z_C: the constants for the specific case of Nafion are $a = 2.71$ and $b = 3.72$. However, we expect these values to change for other systems.

Table 7. Database of selectivity coefficients for several proton/cation combinations in Nafion using Okada's measure (equation (16)) and Steck's reporting convention (at $x_H^m = 0.5$).

Monovalent	Selectivity Coefficient	Divalent	Selectivity Coefficient	Trivalent	Selectivity Coefficient
H^+/Li^+	1.7570	H^+/Mg^{2+}	0.0464	H^+/Al^{3+}	0.0009
H^+/Na^+	0.8887	H^+/Ca^{2+}	0.0289	H^+/Fe^{2+}	0.003
H^+/K^+	0.3069	H^+/Sr^{2+}	0.0177	H^+/V^{2+}	0.1008
H^+/Rb^+	0.2282	H^+/Ba^{2+}	0.0119		
H^+/Cs^+	0.1522	H^+/Ni^{2+}	0.0274		
H^+/Tl^+	0.2806	H^+/Cu^{2+}	0.0296		
H^+/Ag^+	1.1944	H^+/Zn^{2+}	0.2530		
		H^+/Co^{2+}	0.1548		

General cation-cation selectivity database

Proton was fixed as one of the cations in the analysis of preferential partitioning of binary cations into Nafion membranes above given its special status in the field of PEMFCs and electrolyzers. It is worth reiterating that this analysis can be applied to any application that is concerned with binary cation partitioning into Nafion or other exchange membranes, irrespective of whether or not it involves protons. For instance, water purification and desalination applications that employ ionomer membranes may have varied mixes of cations.[20] The extended database of studies involving a broader set of cations is included in the SI for the interested reader and compiled into Table S4. For the incomplete data set, interconversion between different selectivity measures for a small sample of cations was attempted with some success. The same discrepancies, namely differing interpretations of what concentration means in a solid exchanger with discrete charged sites, different selectivity expressions to quantify preferential partitioning, different treatments of selectivity as a function of concentration, etc. plague the partitioning literature beyond protons, Nafion, ionomers, and PEMFC applications. A specific challenge to create a database, however, was the limited overlap of cations studied across studies for the same Nafion membrane type.

SUMMARY AND OUTLOOK

We explicitly stated the conditions of thermodynamic phase equilibrium to revisit the theoretical origins of binary selectivity coefficient and its relationship with ion-partition coefficients within the context of ion-conduction polymers (ionomers). Combined with Figure 1, the aim of this exercise was to re-establish a connection between the concept of selective partitioning and its underlying mathematics. A few common assumptions such as use of unmeasurable single-ion activity coefficients were addressed to instead arrive at a thermodynamically rigorous expression for selectivity coefficient in equation (14). The assumption of Donnan co-ion exclusion should also be relaxed in future works. The

prototypical case of cations partitioning into Nafion was chosen for an illustrative review and example. This analysis reminded us that phase nonideality, cation dissimilarity, and inability of certain ions to cross phase boundary culminate in preferential partitioning of cations from one phase to another.

One of the major concerns of this paper was to expose nuances hidden in processing and interpretation of experimental partitioning data to foster standardization of selectivity values reported in Nafion literature. The main dimensions along which reconciliation was implemented are encapsulated as follows:

- Concentration measures for expressing quantities of ionic species in the ionomer phase: a wide variety ranging from bulk to local and superficial to interstitial measures. The right choice of measure in the model should be commensurate with the accompanying experimental technique as well as the objective of the analysis.
- Definitions of selectivity coefficients: combination of different ways of imagining the ion-exchange reaction, the concentration measure used, and the inclusion or exclusion of phase nonideality via activity coefficients produces the differences in reported selectivity values. In Table 4, a scheme was developed to allow interconversion among these different measures, which is amenable to the general class of electrolytes in contact with ionomers.
- Composition dependence of selectivity coefficients: unlike true equilibrium constants, selectivity coefficients are functions of composition that makes it challenging to characterize the system with a single coefficient value. Various conventions used to report a single-valued selectivity coefficient were discussed and compared. It was seen that the differences between conventions amplified with valences of the cations.

We belabored a consistent quantification measure because it will promote a more transparent comparison between the score of materials employed for any given application. The detailed breakdown of arriving at internally consistent selectivity coefficients from different experimental data sets enabled us to construct a comprehensive cation selectivity database for Nafion, as seen in Table 7. This database can now be used as a reference to enable future researchers to make more informed choices about their experiments and models. A similar database can be valuable for other electrochemical systems such as redox flow batteries and electrolyzers where multiple cations compete for uptake into and transport across the ionomer.

We utilized the cation selectivity database in a correlation study that examined the possibility of estimating selectivity of Nafion towards a given cation versus protons with knowledge of some of this cation's fundamental properties. A brief survey of the models providing expressions for species activity coefficients in the solution and membrane phases allowed the identification of some relevant cation fundamental properties. Although data for multivalent cations is severely lacking to draw conclusions, we were able to draw preliminary correlations for monovalent and divalent cations suggesting that a combination of cation valence and unsolvated ionic radius may be sufficient to obtain a qualitative estimate of Nafion's cation selectivity. The present study can, however, be extended along multiple dimensions including the effect of considering different membrane properties such as ionomer chemistry, ion-exchange capacity, and thicknesses, exploring different ion properties such as ion-aggregation states, cation-pairs, and anion-types, as well as establishing the impact of operating conditions such as temperature on ion exchange.

Revisiting the first principles of the ion-exchange phenomenon as well as standardization of its quantifying measure will help make the research path ahead smoother. In turn, evolving applications are offering fodder for the expansion of ion-exchange research. Proton-exchange-membrane fuel cell technology is at a mature stage with commercialization-related concerns such as cost and durability taking centerstage. Cation uptake by Nafion, or similar class of ionomers for that matter, plays an important role in both these concerns: cations from Pt-alloys used to mitigate catalyst cost can leach as impurities into the MEA and cations can act as radical scavengers for species causing chemical degradation of ionomers. Simultaneous developments in the fields of imaging have made it possible to visualize the *operando* behavior of these cations providing a further boost to multi-ion sorption and transport research in ionomers. Therefore, there is a need to characterize ternary (or even higher level) selectivity coefficients to describe simultaneous uptake of multiple ions into ionomers. With the emergence of alternative ionomers with chemistry or cation-doping modifications and the need for their characterization, it will be more important to accurately quantify selectivity measures of ionomers as performance indicators to allow for materials comparisons and screening. Modern capabilities are also allowing the fabrication and characterization of ever thinner ionomer films thereby engendering a gap in the understanding of species/species interactions in these novel materials in the presence of confinement effects. Thin-film studies will require a re-imagining of the species-species interactions that form the basis of thermodynamic models for ion-sorption.

AUTHOR INFORMATION

Corresponding Authors

Adam Z. Weber – Lawrence Berkeley National Laboratory, 1 Cyclotron Rd, Berkeley, California, USA 94720
Email: azweber@lbl.gov
Ahmet Kusoglu – Lawrence Berkeley National Laboratory, 1 Cyclotron Rd, Berkeley, California, USA 94720

Email: akusoglu@lbl.gov

Authors
Priyamvada Goyal – Lawrence Berkeley National Laboratory, 1 Cyclotron Rd, Berkeley, California, USA 94720

Biographies

Adam Z. Weber is a Senior Scientist and Energy Conversion Group Leader at Berkeley Lab and ECS Fellow who has worked on understanding hydrogen and fuel cells over the last 20 years with a focus on Multiphysics modelling of the underlying phenomena. He received his PhD from UC Berkeley.

webpage: https://weberlab.lbl.gov/

Ahmet Kusoglu is a Scientist at Berkeley Lab working on mechanochemical characterization of ionomers, composites and soft/hard interfaces for electrochemical energy devices. He holds a PhD from University of Delaware, did his post-doctoral research at LBNL, is the recipient of the Srinivasan Award of the Electrochemical Society and ECS-Toyota Fellowship.
webpage: https://kusoglulab.lbl.gov

Priyamvada Goyal is a postdoctoral researcher at Berkeley Lab focusing on developing models for ionomers that can help analyze multiscale interactions of ions, solvent, and polymer species that are not directly observable. Her PhD thesis from University of Oxford focused on models that coupled transport and mechanics within solid polymers.

Acknowledgements

We would like to acknowledge helpful input and discussions from Dr. Andrew Crothers and funding from the Army Research Office under contract AWD00004718. We would also like to acknowledge Ms. Jennifer Garland for her contributions towards developing the non-linear fit algorithm for the selectivity data.

Supporting Information Available: Section 1 contains expanded form of selectivity interconversion tables: Table S1 contains interconversions among all the representative selectivity measures chosen from literature in Table 4; Table S2 contains interconversions between selectivity measures based on different composition variables; Section 2 focuses on composition dependence of selectivity coefficients: Figure S1 is the graphical representation of the composition dependence and compares different conventions; Table S3 contains the selectivity data represented in Figure S1; Section 3 explores multicollinearity among independent variables considered for the correlations study: Figures S2 and S3 show correlations for ion-solvent properties *via* a heat map and scatterplot fits, respectively; similarly, Figures S4 and S5 show correlations for ion-ion properties *via* a heat map and scatterplot fits, respectively. Section 4 focuses on cation-cation selectivities reported in the literature not involving protons: Table S4 presents the selectivity values of Nafion for monovalent and divalent cations relative to alkali metals such as Li, Na, K, and Cs; Table S5 includes interconversions of selectivity values for a small cation sample from Pintauro to Okada measure with the corresponding errors; Table S6 and Figure S6 compare the selectivities of alkali metal cations relative to Li as reported in literature with the selectivities computed from proton-alkali metal selectivities.

LIST OF SYMBOLS

UNIVERSAL CONSTANTS

F	Faraday's constant [= 96485 C/mol]
R	Gas constant [= 8.314 J/mol/K]

SYSTEM PROPERTIES

c_T	Total molar concentration [mol/m^3]
G	Gibbs free energy [kJ]
I	Ionic strength of solution [mol/m^3]
p	Ambient pressure [Pa]
T	Ambient temperature [K]
Φ	Quasielectrostatic potential [V]

SPECIES PROPERTIES

a_i	Activity of species i
c_i	Molar concentration of species i [mol/m^3]
K_i	Partition coefficient of species i
K_{ij}^{eq}	Ion-exchange equilibrium constant
m_i	Molality of species i [mol/kg]
n_i	Moles of species i [mol]
S_i^j	Binary selectivity coefficient, quantifying selectivity of phase for species i over j
$\acute{V}_i$	Partial molar volume of species i [m^3/mol]
x_i	Cation fraction of species i
y_i	Mole fraction of species i
z_i	Charge number or valence of species i
γ_i	Molar activity coefficient of species i
Γ_i	Molal activity coefficient of species i
Γ_i^y	Mole-fractional activity coefficient of species i
Γ_i^x	Cation-fractional activity coefficient of species i
λ	Membrane water content
μ_i	(Electro)chemical potential of species i [kJ/mol]
μ_i^θ	Standard (electro)chemical potential of species i [kJ/mol]
ν_i	Stoichiometric coefficient of species i in a salt

SUPERSCIPTS: PHASES

m	Membrane phase
s	Solution phase

SUBSCRIPTS: SPECIES

H	Protons/first cation
C	Second cation
A	Anion in the solution phase
B	(Stationary) anion in the membrane phase
0	Water
HA	Neutral salt containing ions H and A
CA	Neutral salt containing ions C and A

SECOND CATION PROPERTIES

ΔH_C^{hyd}	Hydration enthalpy of cation C [kJ]
LAS_C	Lewis acid strength of cation C
r_C	Unsolvated radius of cation C [m]
r_C^{hyd}	Hydrated radius of cation C [m]

References

(1) DuChanois, R. M.; Porter, C. J.; Violet, C.; Verduzco, R.; Elimelech, M. Membrane Materials for Selective Ion Separations at the Water–Energy Nexus. *Advanced Materials* **2021**, *33* (38), 1–18. https://doi.org/10.1002/adma.202101312.

(2) Wang, W.; Zhang, Y.; Tan, M.; Xue, C.; Zhou, W.; Bao, H.; Hon Lau, C.; Yang, X.; Ma, J.; Shao, L. Recent Advances in Monovalent Ion Selective Membranes towards Environmental Remediation and Energy Harvesting. *Sep Purif Technol* **2022**, *297* (May), 121520. https://doi.org/10.1016/j.seppur.2022.121520.

(3) Zhang, X. Selective Separation Membranes for Fractionating Organics and Salts for Industrial Wastewater Treatment: Design Strategies and Process Assessment. *J Memb Sci* **2022**, *643* (October 2021), 120052. https://doi.org/10.1016/j.memsci.2021.120052.

(4) Gao, Y.; Feng, X.; Chang, J.; Long, C.; Ding, Y.; Li, H.; Huang, K.; Liu, B.; Yang, J. Surface Ion Exchange and Targeted Passivation with Cesium Fluoride for Enhancing the Efficiency and Stability of Perovskite Solar Cells. *Appl Phys Lett* **2022**, *121*, 073902. https://doi.org/10.1063/5.0097939.

(5) Walsh, A.; Stranks, S. D. Taking Control of Ion Transport in Halide Perovskite Solar Cells. *ACS Energy Lett* **2018**, *3* (8), 1983–1990. https://doi.org/10.1021/acsenergylett.8b00764.

(6) Li, N.; Araya, S. S.; Cui, X.; Kær, S. K. The Effects of Cationic Impurities on the Performance of Proton Exchange Membrane Water Electrolyzer. *J Power Sources* **2020**, *473* (June), 2–9. https://doi.org/10.1016/j.jpowsour.2020.228617.

(7) Hren, M.; Božič, M.; Fakin, D.; Kleinschek, K. S.; Gorgieva, S. Alkaline Membrane Fuel Cells: Anion Exchange Membranes and Fuels. *Sustain Energy Fuels* **2021**, *5* (3), 604–637. https://doi.org/10.1039/d0se01373k.

(8) Pintauro, P. N. Perspectives on Membranes and Separators for Electrochemical Energy Conversion and Storage Devices. *Polymer Reviews* **2015**, *55* (2), 201–207. https://doi.org/10.1080/15583724.2015.1031378.

(9) Laio, A.; Torre, V. Physical Origin of Selectivity in Ionic Channels of Biological Membranes. *Biophys J* **1999**, *76* (1 I), 129–148. https://doi.org/10.1016/S0006-3495(99)77184-5.

(10) Eisenman, G. Cation Selective Glass Electrodes and Their Mode of Operation. *Biophys J* **1962**, *2* (2), 259–323.

(11) Tournassat, C.; Gailhanou, H.; Crouzet, C.; Braibant, G.; Gautier, A.; Gaucher, E. C. Cation Exchange Selectivity Coefficient Values on Smectite and Mixed-Layer Illite/Smectite Minerals. *Soil Science Society of America Journal* **2009**, *73* (3), 928–942. https://doi.org/10.2136/sssaj2008.0285.

(12) Perry, M. L.; Weber, A. Z. Advanced Redox-Flow Batteries: A Perspective. *J Electrochem Soc* **2016**, *163* (1), A5064–A5067. https://doi.org/10.1149/2.0101601jes.

(13) Elgammal, R. A.; Tang, Z.; Sun, C. N.; Lawton, J.; Zawodzinski, T. A. Species Uptake and Mass Transport in Membranes for Vanadium Redox Flow Batteries. *Electrochim Acta* **2017**, *237*, 1–11. https://doi.org/10.1016/j.electacta.2017.03.131.

(14) Lawton, J. S.; Jones, A. M.; Tang, Z.; Lindsey, M.; Zawodzinski, T. Ion Effects on Vanadium Transport in Nafion Membranes for Vanadium Redox Flow Batteries. *J Electrochem Soc* **2017**, *164* (13), A2987–A2991. https://doi.org/10.1149/2.1791712jes.

(15) Leo, A.; Hansch, C.; Elkins, D. Partition Coefficients and Their Uses. *Chem Rev* **1971**, *71* (6), 525–616. https://doi.org/10.1021/cr60274a001.

(16) Dearden, J. C.; Bresnen, G. M. The Measurement of Partition Coefficients. *Quantitative Structure-Activity Relationships* **1988**, *7* (3), 133–144. https://doi.org/10.1002/qsar.19880070304.

(17) Hongsirikarn, K.; Goodwin Jr, J. G.; Greenway, S.; Creager, S. Effect of Cations (Na+, Ca2+, Fe3+) on the Conductivity of a Nafion Membrane. *J Power Sources* **2010**, *195* (21), 7213–7220. https://doi.org/10.1016/j.jpowsour.2010.05.005.

(18) Okada, T.; Nakamura, N.; Yuasa, M.; Sekine, I. Ion and Water Transport Characteristics in Membranes for Polymer Electrolyte Fuel Cells Containing H+ and Ca2+ Cations. *J Electrochem Soc* **1997**, *144* (8), 2744–2750. https://doi.org/10.1149/1.1837890.

(19) Steck, A.; Yeager, H. L. Water Sorption and Cation-Exchange Selectivity of a Perfluorosulfonate Ion-Exchange Polymer. *Anal Chem* **1980**, *52* (8), 1215–1218. https://doi.org/10.1021/ac50058a013.

(20) Luo, T.; Abdu, S.; Wessling, M. Selectivity of Ion Exchange Membranes: A Review. *J Memb Sci* **2018**, *555* (December 2017), 429–454. https://doi.org/10.1016/j.memsci.2018.03.051.

(21) Stenina, I.; Golubenko, D.; Nikonenko, V.; Yaroslavtsev, A. Selectivity of Transport Processes in Ion-Exchange Membranes: Relationship with the Structure and Methods for Its Improvement. *Int J Mol Sci* **2020**, *21* (15), 1–33. https://doi.org/10.3390/ijms21155517.

(22) Kusoglu, A.; Weber, A. Z. New Insights into Perfluorinated Sulfonic-Acid Ionomers. *Chem Rev* **2017**, *117* (3), 987–1104. https://doi.org/10.1021/acs.chemrev.6b00159.

(23) Kamcev, J.; Freeman, B. D. Charged Polymer Membranes for Environmental/Energy Applications. *Annu Rev Chem Biomol Eng* **2016**, *7* (March), 111–133. https://doi.org/10.1146/annurev-chembioeng-080615-033533.

(24) Jiang, S.; Sun, H.; Wang, H.; Ladewig, B. P.; Yao, Z. A Comprehensive Review on the Synthesis and Applications of Ion Exchange Membranes. *Chemosphere* **2021**, *282*, 130817. https://doi.org/10.1016/j.chemosphere.2021.130817.

(25) Ran, J.; Wu, L.; He, Y.; Yang, Z.; Wang, Y.; Jiang, C.; Ge, L.; Bakangura, E.; Xu, T. Ion Exchange Membranes: New Developments and Applications. *J Memb Sci* **2017**, *522*, 267–291. https://doi.org/10.1016/j.memsci.2016.09.033.

(26) Kundu, P. P.; Pal, A. Cation Exchange Polymeric Membranes for Fuel Cells. *Reviews in Chemical Engineering* **2006**, *22* (3), 125–153. https://doi.org/10.1515/REVCE.2006.22.3.125.

(27) Peighambardoust, S. J.; Rowshanzamir, S.; Amjadi, M. *Review of the Proton Exchange Membranes for Fuel Cell Applications*; Elsevier Ltd, 2010; Vol. 35. https://doi.org/10.1016/j.ijhydene.2010.05.017.

(28) Cullen, D. A.; Neyerlin, K. C.; Ahluwalia, R. K.; Mukundan, R.; More, K. L.; Borup, R. L.; Weber, A. Z.; Myers, D. J.; Kusoglu, A. New Roads and Challenges for Fuel Cells in Heavy-Duty Transportation. *Nat Energy* **2021**, *6* (5), 462–474. https://doi.org/10.1038/s41560-021-00775-z.

(29) Holdcroft, S. Fuel Cell Catalyst Layers: A Polymer Science Perspective. *Chemistry of Materials* **2014**, *26* (1), 381–393. https://doi.org/10.1021/cm401445h.

(30) Kushner, D. I.; Crothers, A. R.; Kusoglu, A.; Weber, A. Z. Transport Phenomena in Flow Battery Ion-Conducting Membranes. *Curr Opin Electrochem* **2020**, *21*, 132–139. https://doi.org/10.1016/j.coelec.2020.01.010.

(31) Zatoń, M.; Prélot, B.; Donzel, N.; Rozière, J.; Jones, D. J. Migration of Ce and Mn Ions in PEMFC and Its Impact on PFSA Membrane Degradation. *J Electrochem Soc* **2018**, *165* (6), F3281–F3289. https://doi.org/10.1149/2.0311806jes.

(32) Tesfaye, M.; Kusoglu, A. Impact of Co-Alloy Leaching and Cation in Ionomer Thin-Films. *ECS Trans* **2018**, *86* (13), 359–367. https://doi.org/10.1149/08613.0359ecst.

(33) Lee, C. H.; Wang, X.; Peng, J. K.; Katzenberg, A.; Ahluwalia, R. K.; Kusoglu, A.; Komini Babu, S.; Spendelow, J. S.; Mukundan, R.; Borup, R. L. Toward a Comprehensive Understanding of Cation Effects in Proton Exchange Membrane Fuel Cells. *ACS Appl Mater Interfaces* **2022**, *14* (31), 35555–35568. https://doi.org/10.1021/acsami.2c07085.

(34) Zatoń, M.; Rozière, J.; Jones, D. J. Mitigation of PFSA Membrane Chemical Degradation Using Composite Cerium Oxide-PFSA Nanofibres. *J Mater Chem A Mater* **2017**, *5* (11), 5390–5401. https://doi.org/10.1039/c6ta10977b.

(35) Danilczuk, M.; Schlick, S.; Coms, F. D. Cerium(III) as a Stabilizer of Perfluorinated Membranes Used in Fuel Cells: In Situ Detection of Early Events in the ESR Resonator. *Macromolecules* **2009**, *42* (22), 8943–8949. https://doi.org/10.1021/ma9017108.

(36) Fan, J.; Chen, M.; Zhao, Z.; Zhang, Z.; Ye, S.; Xu, S.; Wang, H.; Li, H. Bridging the Gap between Highly Active Oxygen Reduction Reaction Catalysts and Effective Catalyst Layers for Proton Exchange Membrane Fuel Cells. *Nat Energy* **2021**, *6* (5), 475–486. https://doi.org/10.1038/s41560-021-00824-7.

(37) Baker, A. M.; Crothers, A. R.; Chintam, K.; Luo, X.; Weber, A. Z.; Borup, R. L.; Kusoglu, A. Morphology and Transport of Multivalent Cation-Exchanged Ionomer Membranes Using Perfluorosulfonic Acid-Cez+ as a Model System. *ACS Appl Polym Mater* **2020**, *2* (8), 3642–3656. https://doi.org/10.1021/acsapm.0c00633.

(38) Sulek, M. S.; Mueller, S. A.; Paik, C. H. Impact of Pt and Pt-Alloy Catalysts on Membrane Life in PEMFCs. *Electrochemical and Solid-State Letters* **2008**, *11* (5). https://doi.org/10.1149/1.2889000.

(39) Okada, T.; Ayato, Y.; Yuasa, M.; Sekine, I. The Effect of Impurity Cations on the Transport Characteristics of Perfluorosulfonated Ionomer Membranes. *Journal of Physical Chemistry B* **1999**, *103* (17), 3315–3322. https://doi.org/10.1021/jp983762d.

(40) Huang, K. L.; Holsen, T. M.; Selman, J. R. Impurity Partitioning in Nafion and Ceramic Separators Used for Purification of Spent Chromium Plating Solutions. *J Memb Sci* **2002**, *210* (1), 137–145. https://doi.org/10.1016/S0376-7388(02)00384-8.

(41) Shi, S.; Weber, A. Z.; Kusoglu, A. Structure-Transport Relationship of Perfluorosulfonic-Acid Membranes in Different Cationic Forms. *Electrochim Acta* **2016**, *220*, 517–528. https://doi.org/10.1016/j.electacta.2016.10.096.

(42) Goswami, A. K.; Acharya, A.; Pandey, A. K. Study of Self-Diffusion of Monovalent and Divalent Cations in Nafion-117 Ion-Exchange Membrane. *Journal of Physical Chemistry B* **2001**, *105* (38), 9196–9201. https://doi.org/10.1021/jp010529y.

(43) Yoshida, H.; Miura, Y. Behavior of Water in Perfluorinated Ionomer Membranes Containing Various Monovalent Cations. *J Memb Sci* **1992**, *68* (1–2), 1–10. https://doi.org/10.1016/0376-7388(92)80145-A.

(44) Donnan, F. G. Theory of Membrane Equilibria and Membrane Potentials in the Presence of Non-Dialysing Electrolytes. A Contribution to Physical-Chemical Physiology. *J Memb Sci* **1995**, *100* (1), 45–55. https://doi.org/10.1016/0376-7388(94)00297-C.

(45) Okada, T.; Satou, H.; Okuno, M.; Yuasa, M. Ion and Water Transport Characteristics of Perfluorosulfonated Ionomer Membranes with H+ and Alkali Metal Cations. *Journal of Physical Chemistry B* **2002**, *106* (6), 1267–1273. https://doi.org/10.1021/jp013195l.

(46) Yeager, H. L.; Steck, A. Ion-Exchange Selectivity and Metal Ion Separations with a Perfluorinated Cation-Exchange Polymer. *Anal Chem* **1979**, *51* (7), 862–865. https://doi.org/10.1021/ac50043a020.

(47) Palomo, J.; Pintauro, P. N. Competitive Absorption of Quaternary Ammonium and Alkali Metal Cations into a Nafion Cation-Exchange Membrane. *J Memb Sci* **2003**, *215* (1–2), 103–114. https://doi.org/10.1016/S0376-7388(02)00606-3.

(48) Pintauro, P. N.; Bontha, J. R. Water Orientation and Ion Solvation Effect during Multicomponent Salt Partitioning in a Nafion Cation Exchange Membrane. *Chem Eng Sci* **1994**, *49* (23), 3835–3851.

(49) Crothers, A. R.; Darling, R. M.; Kusoglu, A.; Radke, C. J.; Weber, A. Z. Theory of Multicomponent Phenomena in Cation-Exchange Membranes: Part I. Thermodynamic Model and Validation. *J Electrochem Soc* **2020**, *167* (1), 013547. https://doi.org/10.1149/1945-7111/ab6723.

(50) Sujanani, R.; Katz, L. E.; Paul, D. R.; Freeman, B. D. Aqueous Ion Partitioning in Nafion: Applicability of Manning's Counter-Ion Condensation Theory. *J Memb Sci* **2021**, *638* (May), 119687. https://doi.org/10.1016/j.memsci.2021.119687.

(51) Gibbs, J. W. *The Collected Works of J. Willard Gibbs Volume I Thermodynamics*; 1928. https://doi.org/10.1201/b12732-15.

(52) Gaines, G. L.; Thomas, H. C. Adsorption Studies on Clay Minerals. II. A Formulation of the Thermodynamics of Exchange Adsorption. *J Chem Phys* **1953**, *21* (4), 714–718. https://doi.org/10.1063/1.1698996.

(53) Holt, T.; Førland, T.; Ratkje, S. K. Cation Exchange Membranes as Solid Solutions. *J Memb Sci* **1985**, *25* (2), 133–151. https://doi.org/10.1016/S0376-7388(00)80247-1.

(54) Meares, P.; Thain, J. F. The Thermodynamics of Cation Exchange. VI. Selectivity and Activity Coefficients in Moderately Concentrated Solutions. *Journal of Physical Chemistry* **1968**, *72* (8), 2789–2797. https://doi.org/10.1021/j100854a017.

(55) Högfeldt, E. A Useful Method for Summarizing Data in Ion Exchange. I. Some Illustrative Examples. *Reactive Polymers, Ion Exchangers, Sorbents* **1984**, *2* (1–2), 19–30. https://doi.org/10.1016/0167-6989(84)90005-9.

(56) Guggenheim, E. A. The Conceptions of Electrical Potential Difference between Two Phases and the Individual Activities of Ions. *Journal of Physical Chemistry* **1929**, *33* (6), 842–849. https://doi.org/10.1021/j150300a003.

(57) Lewis, G. N.; Randall, M. The Activity Coefficient of Strong Electrolytes. *J Am Chem Soc* **1921**, *43* (5), 1112–1154. https://doi.org/10.1021/ja01438a014.

(58) Pitzer, K. S. *Activity Coefficients in Electrolyte Solutions*; 2018. https://doi.org/10.1201/9781351069472.

(59) Newman, J.; Balsara, N. P. *Electrochemical Systems*, 4th ed.; John Wiley & Sons Inc.: Hoboken, NJ, 2021. https://doi.org/10.1007/978-94-007-2999-5_11.

(60) Goyal, P.; Monroe, C. W. Thermodynamic Factors for Locally Non-Neutral, Concentrated Electrolytic Fluids. *Electrochim Acta* **2021**, *371*, 137638. https://doi.org/10.1016/j.electacta.2020.137638.

(61) Smyrl, W. H.; Newman, J. Potentials of Cells with Liquid Junctions. *Journal of Physical Chemistry* **1968**, *72* (13), 4660–4671. https://doi.org/10.1021/j100859a051.

(62) Gao, K. W.; Yu, X.; Darling, R. M.; Newman, J.; Balsara, N. P. Increased Donnan Exclusion in Charged Polymer Networks at High Salt Concentrations. *Soft Matter* **2022**, *18* (2), 282–292. https://doi.org/10.1039/d1sm01511g.

(63) Savage, J.; Tse, Y. S.; Voth, G. A. Proton Transport Mechanism of Perfluorosulfonic Acid Membranes. *The Journal of Physical Chemistry C* **2014**, *118*, 17436–17445. https://doi.org/10.1021/jp504714d.

(64) Crothers, A. R.; Radke, C. J.; Weber, A. Z. Impact of Nano- and Mesoscales on Macroscopic Cation Conductivity in Perfluorinated-Sulfonic-Acid Membranes. *The Journal of Physical Chemistry C* **2017**, *121*, 28262–28274. https://doi.org/10.1021/acs.jpcc.7b07360.

(65) Manning, M. J.; Meleheimer, S. S. Binary and Ternary Ion-Exchange Equilibria with a Perfluorosulfonic Acid Membrane. *Industrial and Engineering Chemistry Fundamentals* **1983**, *22* (3), 311–317. https://doi.org/10.1021/i100011a008.

(66) Kyllönen, J.; Hakanen, M.; Lindberg, A.; Harjula, R.; Vehkamäki, M.; Lehto, J. Modeling of Cesium Sorption on Biotite Using Cation Exchange Selectivity Coefficients. *Radiochim Acta* **2014**, *102* (10), 919–929. https://doi.org/10.1515/ract-2013-2180.

(67) Visconti, F.; de Paz, J. M.; Rubio, J. L. Choice of Selectivity Coefficients for Cation Exchange Using Principal Components Analysis and Bootstrap Anova of Coefficients of Variation. *Eur J Soil Sci* **2012**, *63* (4), 501–513. https://doi.org/10.1111/j.1365-2389.2012.01474.x.

(68) Tandon, R.; Pintauro, P. N. Divalent/Monovalent Cation Uptake Selectivity in a Nafion Cation-Exchange Membrane: Experimental and Modeling Studies. *J Memb Sci* **1997**, *136* (1–2), 207–219. https://doi.org/10.1016/S0376-7388(97)00167-1.

(69) Crothers, A. R.; Darling, R. M.; Kusoglu, A.; Radke, C. J.; Weber, A. Z. Theory of Multicomponent Phenomena in Cation-Exchange Membranes: Part II. Transport Model and Validation. *J Electrochem Soc* **2020**, *167* (1), 013548. https://doi.org/10.1149/1945-7111/ab6724.

(70) Peng, J.; Tian, M.; Cantillo, N. M.; Zawodzinski, T. The Ion and Water Transport Properties of K+ and Na+ Form Perfluorosulfonic Acid Polymer. *Electrochim Acta* **2018**, *282*, 544–554. https://doi.org/10.1016/j.electacta.2018.06.035.

(71) Szentirmay, M. N.; Martin, C. R. Ion-Exchange Selectivity of Nafion Films on Electrode Surfaces. *Anal Chem* **1984**, *56* (11), 1898–1902. https://doi.org/10.1021/ac00275a031.

(72) Miyoshi, H.; Yamagami, M.; Kataoka, T. Influence of the Concentration of Ions in Solution on the Partition Coefficient between Cation Exchange Membrane and Solution. *Solvent Extraction and Ion Exchange* **1993**, *11* (3), 505–520. https://doi.org/10.1080/07366299308918170.

(73) Myers, G. E.; Boyd, G. E. A Thermodynamic Calculation of Cation Exchange Selectivities. *Journal of Physical Chemistry* **1956**, *60* (5), 521–529. https://doi.org/10.1021/j150539a003.

(74) Bonner, O. D.; Smith, L. lou. A Selectivity Scale for Some Divalent Cations on Dowex 50. *Journal of Physical Chemistry* **1957**, *61* (3), 326–329. https://doi.org/10.1021/j150549a011.

(75) Karnland, O.; Birgersson, M.; Hedström, M. Selectivity Coefficient for Ca/Na Ion Exchange in Highly Compacted Bentonite. *Physics and Chemistry of the Earth* **2011**, *36* (17–18), 1554–1558. https://doi.org/10.1016/j.pce.2011.07.023.

(76) Braaten, J. P.; Xu, X.; Cai, Y.; Kongkanand, A.; Litster, S. Contaminant Cation Effect on Oxygen Transport through the Ionomers of Polymer Electrolyte Membrane Fuel Cells. *J Electrochem Soc* **2019**, *166* (16), F1337–F1343. https://doi.org/10.1149/2.0671916jes.

(77) Prakash, P.; Sengupta, A. K. Modeling Al3+/H+ Ion Transport in Donnan Membrane Process for Coagulant Recovery. *AIChE Journal* **2005**, *51* (1), 333–344. https://doi.org/10.1002/aic.10312.

(78) Pintauro, P. N.; Tandon, R.; Chao, L.; Xu, W.; Evilia, R. Equilibrium Partitioning of Monovalent/Bivalent Cation-Salt Mixtures in Nafion Cation-Exchange Membranes. *Journal of Physical Chemistry* **1995**, *99* (34), 12915–12924. https://doi.org/10.1021/j100034a034.

(79) Kielland, J. Individual Activity Coefficients of Ions in Aqueous Solutions. *J Am Chem Soc* **1937**, *59* (9), 1675–1678. https://doi.org/10.1021/ja01288a032.

(80) Stokes, R. H.; Robinson, R. A. Ionic Hydration and Activity in Electrolyte Solutions. *J Am Chem Soc* **1948**, *70* (5), 1870–1878. https://doi.org/10.1021/ja01185a065.

(81) Katchalsky, A.; Michaeli, I. Polyelectrolyte Gels in Salt Solutions. *Journal of Polymer Science* **1955**, *15* (79), 69–86. https://doi.org/10.1002/pol.1955.120157906.

(82) Peng, J.; Zawodzinski, T. A. Describing Ion Exchange Membrane-Electrolyte Interactions for High Electrolyte Concentrations Used in Electrochemical Reactors. *J Memb Sci* **2020**, *593* (March 2019), 117340. https://doi.org/10.1016/j.memsci.2019.117340.

(83) Kitto, D.; Kamcev, J. Manning Condensation in Ion Exchange Membranes: A Review on Ion Partitioning and Diffusion Models. *Journal of Polymer Science* **2022**, No. November 2021, 1–45. https://doi.org/10.1002/pol.20210810.

(84) Sujanani, R.; Katz, L. E.; Paul, D. R.; Freeman, B. D. Aqueous Ion Partitioning in Nafion: Applicability of Manning's Counter-Ion Condensation Theory. *J Memb Sci* **2021**, *638* (May), 119687. https://doi.org/10.1016/j.memsci.2021.119687.

(85) Hartman, P.; Chan, H. K. Application of the Periodic Bond Chain (PBC) Theory and Attachment Energy Consideration to Derive the Crystal Morphology of Hexamethylmelamine. *Pharmaceutical Research: An Official Journal of the American Association of Pharmaceutical Scientists* **1993**, *10* (7), 1052–1058. https://doi.org/10.1023/A:1018927109487.

(86) Marcus, Y. Thermodynamics of Solvation of Ions. *Journal of Chemical Society Faraday Transactions* **1991**, *87* (18), 2995–2999. https://doi.org/10.1088/1751-8113/44/8/085201.

(87) Smith, D. W. *Inorganic Substances: A Prelude to the Study of Descriptive Inorganic Chemistry*; Cambridge University Press, 1990; Vol. 28. https://doi.org/10.5860/choice.28-0302.

(88) Brown, I. D. What Factors Determine Cation Coordination Numbers? *Acta Crystallographica Section B* **1988**, *44* (6), 545–553. https://doi.org/10.1107/S0108768188007712.

(89) Brown, I. D.; Skowron, A. Electronegativity and Lewis Acid Strength. *J Am Chem Soc* **1990**, *112* (9), 3401–3403. https://doi.org/10.1021/ja00165a023.

(90) Li, K.; Xue, D. Estimation of Electronegativity Values of Elements in Different Valence States. *Journal of Physical Chemistry A* **2006**, *110* (39), 11332–11337. https://doi.org/10.1021/jp062886k.

(91) Li, K.; Li, M.; Xue, D. Solution-Phase Electronegativity Scale: Insight into the Chemical Behaviors of Metal Ions in Solution. *Journal of Physical Chemistry A* **2012**, *116* (16), 4192–4198. https://doi.org/10.1021/jp300603f.

Table of Contents Graphic:

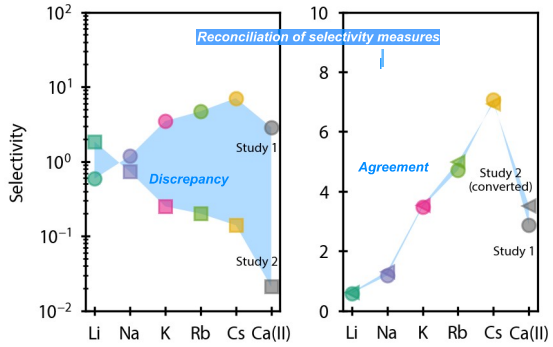

Quotes to be highlighted:

This paper aims to amalgamate the various theoretical approaches to quantify selectivity coefficients across literature so that the existing as well as new experimental data on Nafion cation selectivity can be processed together into one consistent database, paving the way to extend this methodology to other materials.

One of the peculiarities in reporting a selectivity coefficient in general is that, unlike an equilibrium constant, which is a fixed value at a given temperature, the selectivity coefficient often tends to vary with species composition.

A major challenge in reviewing ion-partitioning literature lies in reconciling the various measures used to quantify it, with the similarities in approaches further obscured by incompatible and inconsistent terminology.

Although data for multivalent cations is severely lacking to draw conclusions, we were able to draw preliminary correlations for monovalent and divalent cations suggesting that a combination of cation valence and unsolvated ionic radius may be sufficient to obtain a qualitative estimate of Nafion's cation selectivity.